AD-A141 703 LITERATURE SURVEY: BASIC MECHANISMS OF EXPLOSIVE COMPOUNDS IN WASTEWATER(U) SUMX CORP AUSTIN TX D W DEBERRY ET AL. MAY 84 SUMX-C82-121 DRXTH-TE-CR-84279 DAAK11-83-C-0006 1/2

UNCLASSIFIED F/G 13/2 NL

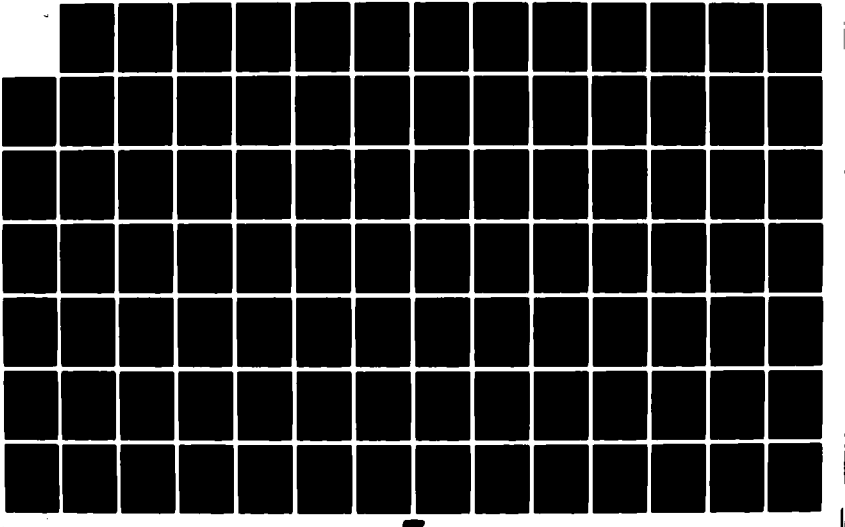

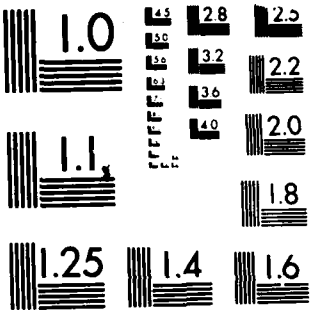

SumX Corporation

SumX No. C82-121

DRXTH-TE-CR-84279

FINAL REPORT

LITERATURE SURVEY:

BASIC MECHANISMS OF EXPLOSIVE COMPOUNDS IN WASTEWATER

Contract Number DAAK11-83-C-0006

Prepared by:

David W. DeBerry
Alfred Viehbeck
Dean Meldrum

May 1984

Distribution Unlimited. Approved for Public Release.

Prepared for:

Cdr., USATHAMA
Aberdeen Proving Ground, Maryland 21010

2211 DENTON DRIVE • P.O. BOX 14864 • AUSTIN, TX 78761 • (512) 835-0330

DISCLAIMER

This Report has been reviewed by the Department of the Army, USATHAMA, and approved for public dissemination. Approval does not signify that the contents necessarily reflect the views and policies of the Army, nor does mention of trade names or commercial products constitute endorsement or recommendation for use.

UNCLASSIFIED

SECURITY CLASSIFICATION OF THIS PAGE (When Data Entered)

REPORT DOCUMENTATION PAGE		READ INSTRUCTIONS BEFORE COMPLETING FORM
1. REPORT NUMBER DRXTH-TE-CR-84279	2. GOVT ACCESSION NO.	3. RECIPIENT'S CATALOG NUMBER
4. TITLE (and Subtitle) BASIC MECHANISMS OF EXPLOSIVE COMPOUNDS IN WASTEWATER		5. TYPE OF REPORT & PERIOD COVERED FINAL 13 Dec. 1982 - 13 Dec. 1983 6. PERFORMING ORG. REPORT NUMBER
7. AUTHOR(s) David W. DeBerry, Alfred Viehbeck and Dean A. Meldrum		8. CONTRACT OR GRANT NUMBER(s) DAAK11-83-C-0006
9. PERFORMING ORGANIZATION NAME AND ADDRESS SumX Corporation P. O. Box 14864, 2211 Denton Drive Austin, Texas 78761		10. PROGRAM ELEMENT, PROJECT, TASK AREA & WORK UNIT NUMBERS
11. CONTROLLING OFFICE NAME AND ADDRESS		12. REPORT DATE May 1984 13. NUMBER OF PAGES 105
14. MONITORING AGENCY NAME & ADDRESS(if different from Controlling Office) USATHAMA Department of the Army Aberdeen Proving Ground, MD 21010		15. SECURITY CLASS. (of this report) UNCLASSIFIED 15a. DECLASSIFICATION/DOWNGRADING SCHEDULE

16. DISTRIBUTION STATEMENT (of this Report)

17. DISTRIBUTION STATEMENT (of the abstract entered in Block 20, if different from Report)

18. SUPPLEMENTARY NOTES

N/A

19. KEY WORDS (Continue on reverse side if necessary and identify by block number)

wastewater treatment, explosive wastes, 2,4,6-trinitrotoluene, 1,3,5-trinitrobenzene, oxidation, photolysis, ozone, hydrogen peroxide, radical intermediates, chemical kinetics

20. ABSTRACT (Continue on reverse side if necessary and identify by block number)

In the production, packing, and demilitarization of TNT large volumes of contaminated water containing from 1 to 150 mg/L of 2,4,6-trinitrotoluene (TNT) may be generated. This project studied the mechanisms of oxidative treatment methods for trinitroaromatic-containing wastewaters. The following methods were examined: (i) hydrogen peroxide photolysis, (ii) direct ozonation, (iii) ozone photolysis, (iv) catalytic ozone-hydrogen peroxide decomposition, and (v) transition metal catalyzed hydrogen peroxide decomposition. The effects

DD FORM 1 JAN 73 1473 EDITION OF 1 NOV 65 IS OBSOLETE

UNCLASSIFIED

SECURITY CLASSIFICATION OF THIS PAGE (When Data Entered)

20. Continued

of solution pH, temperature, and the intensity of ultraviolet light irradiation on the removal of the nitroaromatics were examined. The oxidation of 1,3,5-trinitrobenzene (TNB) was found to be the rate limiting step in the removal of nitroaromatic compounds in TNT-containing waters. Both TNT and TNB in dilute aqueous solution can be removed by methods which generate highly reactive hydroxyl radicals. The ozone photolysis approach is efficient from a reagent usage viewpoint. The combination ozone/hydrogen peroxide catalytic method appears to be an attractive nonphotolytic means of eliminating low concentrations of nitroaromatics in solution.

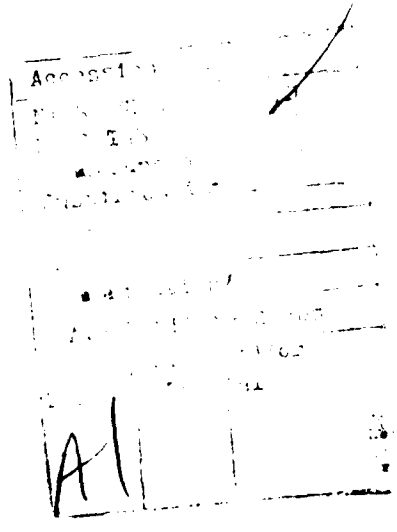

TABLE OF CONTENTS

LIST OF TABLES

LIST OF FIGURES

SECTION 1
INTRODUCTION

This Final Report presents the results of a project conducted by SumX Corporation for the U.S. Army (USATHAMA) entitled "Basic Mechanisms of Explosive Compounds in Wastewater," Contract DAAK11-83-C-0006. In Phase I of this project a literature survey was done by SumX and transmitted as an interim report to THAMA. The present report is concerned with the subsequent Phase II experimental program performed at SumX. This experimental work was done to obtain a better understanding of the oxidative mechanisms involved in the treatment of trinitroaromatic-containing wastewaters. Most of the oxidative treatment processes proposed for cleanup of such streams involve very complex chemical reactions. A more basic understanding of these reactions should allow more effective and efficient treatment programs to be designed.

Several types of wastewater streams are generated during the production, packing, and demilitarization of TNT and related compounds. These streams may contain from 1 to 150 mg/L of TNT, and considerable volumes of contaminated water may be produced. A number of methods have been proposed for cleaning up these streams. One class of methods which has received considerable attention recently involves photooxidation or other means of generating highly reactive oxyradicals which then react with the trinitroaromatic compound to eventually oxidize it to carbon dioxide, water, and inorganic nitrogen species. Such methods are promising since they are often relatively efficient and effective even when the pollutant is present at low concentrations. Their chemistry is quite complicated, however, and difficult to optimize on an engineering scale. The present project was conceived to provide a better fundamental basis for comparison and future optimization of such processes.

The conclusions drawn from this experimental program are summarized in Section 2. They show that a number of areas have been clarified by this study. In addition several new process options including an effective nonphotolytic oxyradical generating reaction have been found. The experimental conditions and techniques employed are given in Section 3. Section 4 then gives the detailed results of the program along with discussion of these results.

SECTION 2
CONCLUSIONS

The primary conclusions obtained in this study are summarized below.

1. Both 2,4,6-trinitrotoluene (TNT) and 1,3,5-trinitrobenzene (TNB) in dilute aqueous solution can be destroyed by techniques which generate highly reactive hydroxyl radicals, i.e., H_2O_2/UV, O_3/UV, and catalyzed nonphotolytic methods.

2. The decompositon of TNB is the rate limiting reaction in the removal of TNT for the processes studied here. (Also see Conclusion 4.)

3. Reaction of TNB with hydroxy radical does not produce long-lived aromatic ring intermediates. Small organic acids are produced which are difficult to oxidize completely.

4. Kinetic analysis of the H_2O_2/UV nitroaromatic systems yielded rate constants of 5.5×10^7 $M^{-1}s^{-1}$ for reaction of TNT with hydroxyl radical, and 1.6×10^7 $M^{-1}s^{-1}$ for reaction of TNB with hydroxyl radical. Results consistent with this were obtained for O_3/UV, which is, however, a more complex system for kinetic analysis.

5. Increasing the reaction temperature from 25° to 70°C did not increase the effectiveness of either the O_3/UV or H_2O_2/UV reactions with trinitroaromatic compounds.

6. The O_3/UV system was relatively insensitive to increasing UV light intensity above a certain threshold value. Considerable oxidation of TNB by O_3 occurred in the dark, in contrast to H_2O_2 which did not oxidize TNB in the dark.

7. The overall reagent usage efficiency of O_3 in O_3/UV systems was much higher than H_2O_2 in H_2O_2/UV systems. This is attributed to the competitive reaction of hydroxyl radical with H_2O_2 in the relatively concentrated H_2O_2 solution. However, high concentrations of H_2O_2 are needed for efficient photlysis due to the low absorbance of H_2O_2. An intermediate concentration of H_2O_2 would be required for optimum overall performance.

8. Changes in system pH from acidic to neutral had only minor effects on the photooxidation efficiency of trinitroaromatics.

9. The H_2O_2/UV attack on trinitroaromatic compounds is accelerated by cupric ion. Reagent consumption is also increased, however. System optimization could lead to an overall improvement over uncatalyzed H_2O_2/UV.

10. Trinitroaromatics can be destroyed by Fenton's reagent (Fe^{2+}/H_2O_2) which is an example of a nonphotolytic method. The attack can be explained by hydroxyl radical formation, however, and no substantial catalysis by iron species was noted.

11. The combination of H_2O_2 and O_3 was found to provide another nonphotolytic method for destruction of low concentrations of nitroaromatics in aqueous systems. This also appears to proceed through a hydroxyl radical intermediate. If optimized, it could provide an attractive alternative to the mechanical (e.g. window fouling) problems inherent in the photochemical processes.

SECTION 3

EXPERIMENTAL METHODS

This section describes the experimental methods and techniques used for this project. The first subsection describes the photochemical reactor used and the associated liquid and gas flow systems. Section 3.2 describes the technique used to measure the UV light intensities. The analytical methods used to follow the course of the reaction and identify the reaction products are described in Section 3.3.

3.1 Reactor and Associated Flow Systems

A bubble column reactor was used during the project. It is shown in Figure 1. It consists of a 22 cm long piece of 2 inch diameter pyrex pipe joined at the bottom with a 2 cm quartz tube which ran the length of the pyrex pipe and acted as a sheath for the ultraviolet lamps. The top of the reactor consisted of a Teflon cap with Viton o-rings and Teflon fittings to allow for the introduction and exhaust of ozone or other gases. The cap was sealed by tightly wrapping Teflon tape around the lip of the reactor and a lip on the lid. The sparger was made from 1/8 inch Teflon tubing which was formed to encircle the quartz sheath at the bottom of the reactor. This sparger had 25 holes 5 mm apart and 0.5 mm in diameter located on the bottom side of the Teflon tubing.

An inlet tube near the top of the reactor and an exit tube fitted with a Teflon stopcock allowed for continuous mixing of the reactor solution by means of a peristaltic pump (Cole Parmer Masterflex with Model 7015.20 head) set at a flow rate of 800 mL/min. The tubing to and from the pump was 1/4 inch standard Teflon tubing with a total length of 2 meters. A 20 cm piece of silicone tubing with an I.D. of 4.8 mm was used in the peristaltic pump.

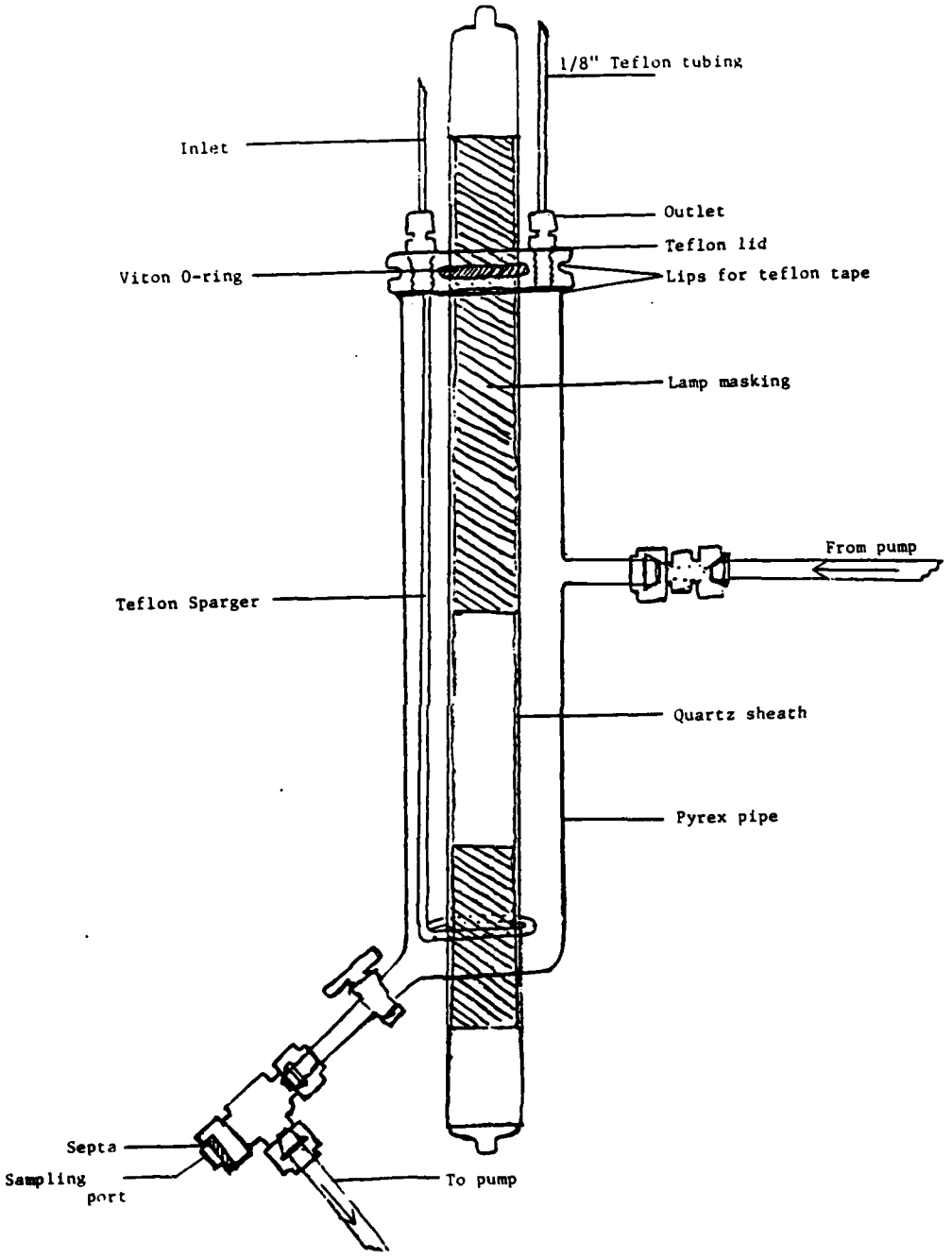

Figure 1. SumX Bubble Column Reactor

The volume of solution in the reactor in all experiments was initially 200 mL. A Teflon tee at the outlet tube was fitted with a Teflon coated septum to allow sampling by syringes of varying sizes. The quartz sheath running through the center of the reactor allowed for UV lamps of various sizes and intensities to be placed in the middle of the reactor. In all cases the light-emitting part of the UV lamps was completely covered by the solution.

When the experiments were not performed with ozone, the sparger was removed, allowing for easier access for filling and cleaning between runs. The pump, flow, and sampling means however, were the same in all of the experiments.

A schematic of the SumX ozonation system is given in Figure 2. Ozone is generated from oxygen using a Union Carbide SG 4060 ozone generator. All transfer lines seeing dry ozone are constructed of either stainless steel, glass or Teflon. Lines seeing wet ozone are either glass or Teflon up to the point of the ozone kill unit at the end of the train. This unit is made of stainless steel tubing wrapped with asbestos insulation and nichrome resistance wire. The temperature is maintained at 350°C.

A transfer line from the ozone generator leads to a glass trap to protect the generator in case of liquid back-up from the experimental system. From the trap a line leads to a Brooks stainless steel rotameter and then to a T-connector with a stainless steel needle valve at both junctions. This system allows for a small stream of ozone to flow to the reactor, while the major portion of the flow necessary to insure proper ozone generator operation and stability may be bypassed directly to the kill unit.

Flow going to the experiment is then directed by a six-port valve to a differential UV-absorbance ozone monitor constructed at SumX

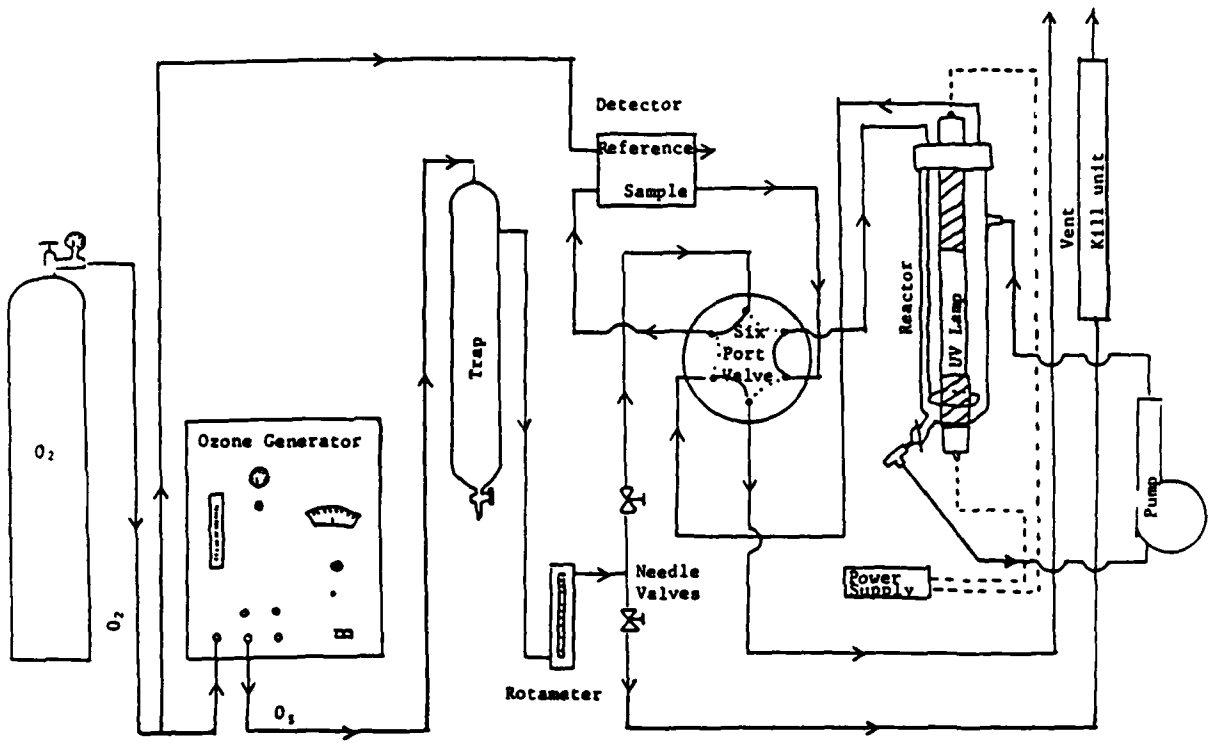

Figure 2. Flow System Diagram.

using silicon UV photovoltaic detector elements (EG&G Electrooptics). The detector was calibrated using Flamm's BKI method (see Section 3.3.2). In the other position the six port valve directs the off-gas from the reactor to the detector for ozone measurement.

3.2 Intensity Measurements

Intensity measurements on the ultraviolet sources used in photooxidation studies were done by means of a potassium ferrioxalate chemical actinometer as described by Hatchand and Parker [1]. Irradiation of the actinometry solution was done in the reactor previously described using the same mixing procedure and sampling techniques. The experiments were conducted in a dark lab to insure the absence of stray light. Nitrogen was blown across the top of the reactor to keep the solution oxygen-free. Samples were taken at zero, 5, and 10 minutes irradiation times.

The lamp used in all of the UV experiments except for the intensity studies was a G10 T 5-1/2L, 5.3 watts, American Ultra-violet Co. lamp. This lamp was masked off to meet the dimensions of the reactor. The lamp's dimensions of 29.2 cm x 4.7 cm and with an advertised output of 5.5 watts was masked to present 7.6 cm x 4.7 cm or 26.3 percent of the total lamp giving a theoretical output of 1.45 watts and a surface area of 35.7 cm^2 or .042 watts/cm^2.

One other source was used without modification (S Hama) Hanamatsu Model No. L937-002. This lamp gave an intensity value of 0.36 watts/0.2 liter and presented a 5.3 cm x 1.9 cm surface to the reactor solution. The S Hama (Tef) was identical lamp with the exception of a Teflon coating heat shrink sheath which absorbed part of the light. Results are summarized below.

TABLE 1. ACTINOMETRY RESULTS

Lamp	I (W/0.2 L)	M-Flux ($Ein \cdot s^{-1}$)	hν Flux/0.2 L (photons s^{-1})
G10 T 5-1/2L	1.31	1.39×10^{-5}	1.67×10^{18}
L. Hama	0.52	5.5×10^{-6}	6.65×10^{17}
S. Hama	0.36	3.8×10^{-6}	4.57×10^{17}
S. Hama (Tef)	0.16	1.69×10^{-6}	2.03×10^{17}

3.3 Analytical Methods

A number of analytical methods were employed during the course of the project. The compounds of interest can be divided into three groups as follows:

1. Organic Nitro Compounds
2. Oxidants
3. Reaction Products.

These topics are discussed below.

3.3.1 Organic Nitro Compounds

Two nitroaromatic compounds were examined as the project progressed: 2,4,6-trinitrotoluene (TNT) and 1,3,5-trinitrobenzene (TNB). The methods used were gas chromatography and a wet chemical method developed at SumX utilizing a Meissenheimer complex.

Gas Chromatography

Standards and samples were extracted with ethyl ether and concentrated by the Kuderna-Danish method. A Varian Model 3700 gas chromatograph with a flame ionization detector (FID) and a Hewlett-Packard 3390A Integrator was used to separate and quantitate the compounds of interest.

A 2 µL sample was injected at an injection temperature of 250°C and at a flow rate of 30 mL/min with nitrogen as the carrier gas. The column was SP 2100 10 percent on 80/100 mesh Chromosorb WHP. The detector temperature 300°C and the oven temperature program was 100° for 6 min., then 10° per minute to 250°.

Sulfite-Meissenheimer Colorimetric Method (SMC)

One unusual feature caused by the low π-electron density of the trinitroaromatic ring is the tendency to formation of "molecular adducts" or "molecular complexes" with electron donor species. these species are often highly colored and stable to some degree in solutions. The adducts formed with anionic species and strong electron donors are often referred to as Meisenheimer complexes. An important structure for the trinitroaromatic forms is the quinoid-type form shown below.

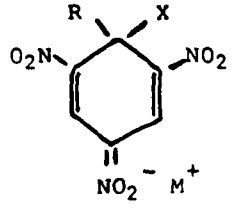

This form results from nucleophilic attack by X, forming an sp^3 type carbon in the ring to which R and X are attached. A more "modern" delocalized form depicting a negative charge associated with

the ring was proposed for a while. However, molecular orbital calculations and crystal structure determinations indicate that most of the negative charge is on the NO_2 group para to the sp^3 carbon, indicating that the form shown above is a more suitable representation.

An analytical method based on the Meissenheimer complex of sulfite with TNT and TNB was developed by SumX Corporation. Solutions containing TNT and TNB were analyzed by GC and SMC to determine applicability within the parameters and conditions of photooxidation experiments. Using a Bausch & Lomb Spectronic 88 Spectrophotometer, the maxima of a known TNT solution complexed with sodium sulfite was determined. This procedure was repeated with TNB and sodium sulfite. The result was a maximum absorbance at 420 nm for the TNT solution and a maximum at 465 for the TNB solution. Standard curves were then run for TNT/TNB mixtures and their slopes determined. Using simultaneous spectrophotometric determination concentrations of both compounds could be determined soon after sampling, using the following equations.

$$C_1 = \frac{(\varepsilon_2)\lambda_2 A\lambda_1 - (\varepsilon_2)\lambda_1 A\lambda_2}{(\varepsilon_1)\lambda_1(\varepsilon_2)\lambda_2 - (\varepsilon_2)\lambda_1(\varepsilon_1)\lambda_2} \quad (1)$$

$$C_2 = \frac{(\varepsilon_1)\lambda_1 A\lambda_2 - (\varepsilon_1)\lambda_2 A\lambda_1}{(\varepsilon_1)\lambda_1(\varepsilon_2)\lambda_2 - (\varepsilon_2)\lambda_1(\varepsilon_1)\lambda_2} \quad (2)$$

When using TNB alone the slope of TNB curve at 465 nm was applied directly. Because of the speed and accuracy of the method during this phase of the project the SMC method became the primary method for determining concentration of TNB in solution. Interference checks were run for the various systems, and gas chromatographic results were used from time to time to verify the SMC results.

3.3.2 Oxidants

Analysis for Hydrogen Peroxide

Two methods were used for determining the concentration of H_2O_2. The primary method was a spectrophotometric method using Ti(IV) [2] and the secondary method boric acid buffered potassium iodide plus ammonium molybdate (BKI/M) [3].

The titanium (IV) method for H_2O_2 analysis was used primarily in this project. This method was standardized by thiosulfate titration and checked against the BKI/M method.

The BKI/M method was used as a check against the TiIV when applicable. This method is an altered iodometric method that was used to determine total oxidants by the addition of ammonium molybdate (0.075 M $(NH_4)_6\ Mo_7 \cdot 4\ H_2O$) in the amount 1 µL/mL.

Analysis for Ozone in Solution

The most specific method used for ozone determinations in solution is that of Hoigne and Bader [4]. The version of the indigo method (HBI) which is used consists of mixing 2 mL of a 1 mM indigo disulfonate solution with 1 mL of phosphate buffer (28 g $NaH_2PO_4 \cdot H_2O$ + 35 g H_3PO_4 diluted to 1 L) and 5 mL of water. To this solution is added 2 mL of ozone water and the absorbance at 610 nm compared to that of a similar solution where the 2 mL of ozone water is replaced by 2 mL of water. The extent of bleaching is proportional to the amount of ozone present.

The classic iodometric method of ozone determination was used to calibrate the ozone in gas monitor (see above). The version (abbreviated BKI) of Flamm's procedure used at SumX is to mix the reagent (0.1 M H_3BO_3/1% KI) with ozone water in a ratio which varies between 10-20

percent ozone water, depending on the suspected concentration. Absorbance of the I_3^- ion is read at 352 nm and compared with a calibration curve prepared by generating known amounts of I_3^- using potassium iodate as a primary standard.

3.3.3 Reaction Products

Organic Acids

Organic acids were determined qualitatively and quantitatively using the benzyl bromide derivatization method of Bethge and Lindstrom [5]. This method is for determining organic acids of low relative molecular mass. The method is based on the conversion of the acids into their benzyl esters via lipophilic tetra-n-butylammonium salts. The benzyl esters are detected and determined by gas chromatography. The GC conditions were as follows:

Varian 3700, Attenuation: 8×10^{-11}, 120°C isothermal, 5.7 percent Sp 1000, 1 µL injection at 200°C with 300°C FID. The solvent was acetone, the flow rate was 30 mL/min and the carrier gas was nitrogen.

Standard curves were run for formic acid and acetic acid and peak areas were integrated by a Hewlett-Packard 3390 A integrator.

Inorganic Nitrate Analysis

Nitrate analyses were conducted on a Dionex Model 16 ion chromatograph at Radian Corporation in Austin. A blind quality control sample was included with the real samples and was correctly analyzed.

Gas Chromatographic/Mass Spectrometry (GC/MS)

GC/MS analyses were conducted on samples extracted and concentrated in ether at Raba-Kistner Consultants, Inc. in San Antonio, Texas. Two chromatographic systems were used for the analyses. One utilized a column fitted with packings with liquid phase of 3 percent SP 2250 on Supelcopak. This system was used to separate neutral and basic organic products. The other system utilized a column fitted with packings with liquid phase of 3 percent SP 1240 DA on Supelocopak. This was a polar liquid phase which was normally employed for the analysis of chlorinated and nitrated-phenols. A diazomethane derivatization procedure was conducted prior to injection on the 1240 column. This method was adopted from "Current Practice in GC-MS Analysis of Organics in Water," EPA-R2-73-277, August, 1973. The gas chromatograph-mass spectrometer unit was a Hewlett-Packard 5992B with a data system 9825 A.

Total Organic Carbon (TOC)

TOC analysis was performed at Aqualab, Inc. in Austin, Texas using a Coulometrics Incorporated Model 5010 TOC analyzer. This instrument used high temperature catalytic oxidation to insure complete conversion of the organic carbon. Samples were acidified and sparged prior to analysis to remove inorganic carbon. Blind quality control samples were included with each sample batch and were correctly analyzed.

SECTION 4
RESULTS AND DISCUSSION

This section presents the experimental results obtained during the program along with pertinent discussion of these results. It begins with a short section describing the photochemistry of the trinitroaromatic substrate compounds in the absence of oxyradicals. This provides baseline information for the rest of the study. The next subsection (4.2) describes the results obtained using photolysis of H_2O_2. This system proved to be the best one for measuring rate constants. Next, the results of the experiments done to characterize the photolytic ozonation of trinitroaromatics is described. This system showed rather high efficiencies for substrate destruction. Finally, nonphotolytic and catalyzed method results are presented in subsection 4.4. A nonphotolytic treatment method was shown to be promising. Also, a transition metal-catalyzed system was demonstrated.

4.1 TNT Photolysis

In view of the fact most nitrobodies, including TNT, absorb radiation at wavelengths in the region where H_2O_2 absorbs, it is important to consider possible direct TNT photochemical interactions and quantum efficiencies. This information is also essential in determining the effect and efficiencies of the photolytic oxidation systems on TNT decomposition.

The photolysis of TNT was carried out under acidic conditions in a solution of 0.01M H_2SO_4 (pH $\sim$ 1.8 $\pm$ 0.1) to examine the direct effect of irradiating with photons having a wavelength of 253.7 nm. Taking the TNT molar absorptivity (ε) value as 3.3×10^3 [6], at a concentration of 0.4 mM, the TNT at this level absorbs $\sim$ 95.2 percent of the incident photons (I°_{254}). The quantum yield (η = moles destroyed/

mole of photons absorbed) for TNT removal through direct photolysis was calculated to be 9×10^{-4}. This value is in agreement with those reported using cyclohexane as solvent [7] but is nearly an order of magnitude lower than those for distilled water [6]. The primary reasons for performing the TNT photolysis experiments was to show the relatively slow direct photolytic decomposition and form a basis for comparing the other decomposition systems. The influence of pH and other conditions were not studied. The influence of direct TNT photolysis was taken as negligible in the systems investigated.

4.2 Hydrogen Peroxide Photolysis

The UV irradiation of hydrogen peroxide in water can cause the cleavage of the oxygen-oxygen bond giving rise to hydroxyl radicals and oxygen molecules. The photodecomposition to hydroxyl radicals after absorption of light at wavelengths up to 365 nm can then be followed by a chain mechanism involving hydroxyl and hydroperoxy radicals [8]. The UV absorption spectrum of H_2O_2 vapor is shown in Figure 3.

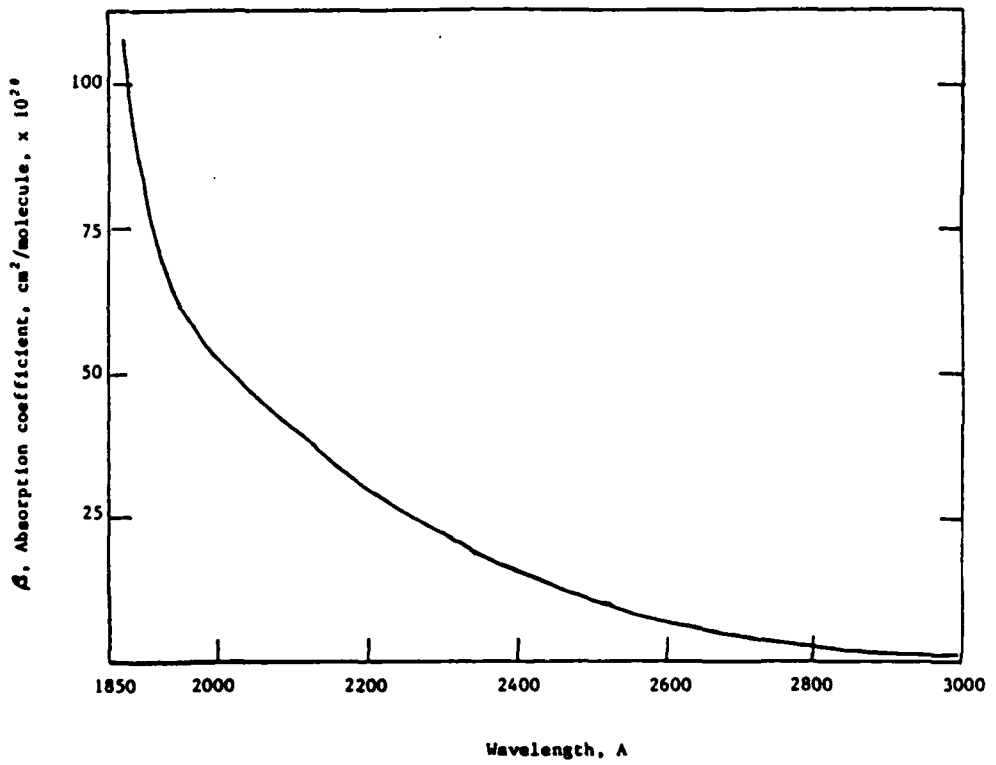

Figure 3. Absorption spectrum of hydrogen peroxide vapor. Taken from [9].

The quantum yields for the production of $HO_2\cdot$ and oxygen during flash photolysis have been determined as 9×10^{-3} and 3×10^{-2} respectively. Hatada et al [10] have reported a quantum yield of 1.84 for scavenged $\cdot OH$ radicals giving a quantum yield for disappearance of H_2O_2 of 0.92. The yield for $\cdot OH$ radicals was a measure of all the $\cdot OH$ radicals which escaped geminate recombination. Molar extinction coefficients for H_2O_2 at 254 and 313 nm were found to be 19 and 0.52 respectively [10]. Thus the absorbance of H_2O_2 is considerably lower than that of ozone. However, much larger concentrations of H_2O_2 than O_3 can be obtained in solution, so that comparable total photolytic absorbances should be possible. Hydrogen peroxide can also be consumed by $\cdot O_2^-$, $HO_2\cdot$ and O_3. It has been shown that the scavenging of radical intermediates (by allyl alcohol) can reduce the quantum yield for H_2O_2 decomposition to nearly 50 percent [9, 11]. Hydroxyl radicals can also be generated from the decomposition of H_2O_2 by transition metal ions as in the Fenton's reagent system which will be examined in the next section.

4.2.1 H_2O_2/UV System

The initial decomposition of H_2O_2 can be accomplished through various means, e.g., using transition metals as catalysts [12] or by UV photodecomposition. A proposed mechanism for H_2O_2 photolysis, involving continued decomposition via chain reactions, is given below.

$$H_2O_2 \xrightleftharpoons{h\nu < 365nm} 2\ OH\cdot \qquad (3)$$

$$H_2O_2 + OH\cdot \longrightarrow H_2O + HO_2\cdot \qquad (4)$$

$$H_2O_2 + HO_2\cdot \longrightarrow H_2O + OH\cdot + O_2 \qquad (5)$$

$$2\ HO_2\cdot \longrightarrow H_2O_2 + O_2 \qquad (6)$$

The photolysis of H_2O_2 at two different concentrations (in the absence of organic substrates) along with the results of a peroxide (blank) run in the dark are shown in Figure 4. The removal data is characteristic of a first-order reaction process. The curves in Figure 4 can be explained using the following simple competion mechanism

Scheme I:

$$H_2O_2 \xrightarrow{k_1} 2\ OH\cdot \qquad (7)$$

$$H_2O_2 + \cdot OH \xrightarrow{k_2} HO_2\cdot + H_2O \qquad k_2 = 3 \times 10^7\ M^{-1}s^{-1}\ [13] \qquad (8)$$

$$2\ HO_2\cdot \xrightarrow{k_3} H_2O_2 + O_2 \qquad k_3 = 8.6 \times 10^5\ M^{-1}s^{-1}[14] \qquad (9)$$

The proposed mechanism is similar to the hydrogen peroxide photolysis mechanism (Eqs. 3-6) above except that it is assumed geminate recombination of hyroxyl radicals is negligible and that Eq. 5 is also negligible since superoxide (in this case the hydrated form at pH < 4.7) reacts much slower than OH· [14]. Adopting the steady-state hypothesis to the hydroperoxy radical ($HO_2^{\cdot}$), its concentration can be expected to remain constant with time or

$$\frac{d(HO_2\cdot)}{dt} = 0 \qquad (10)$$

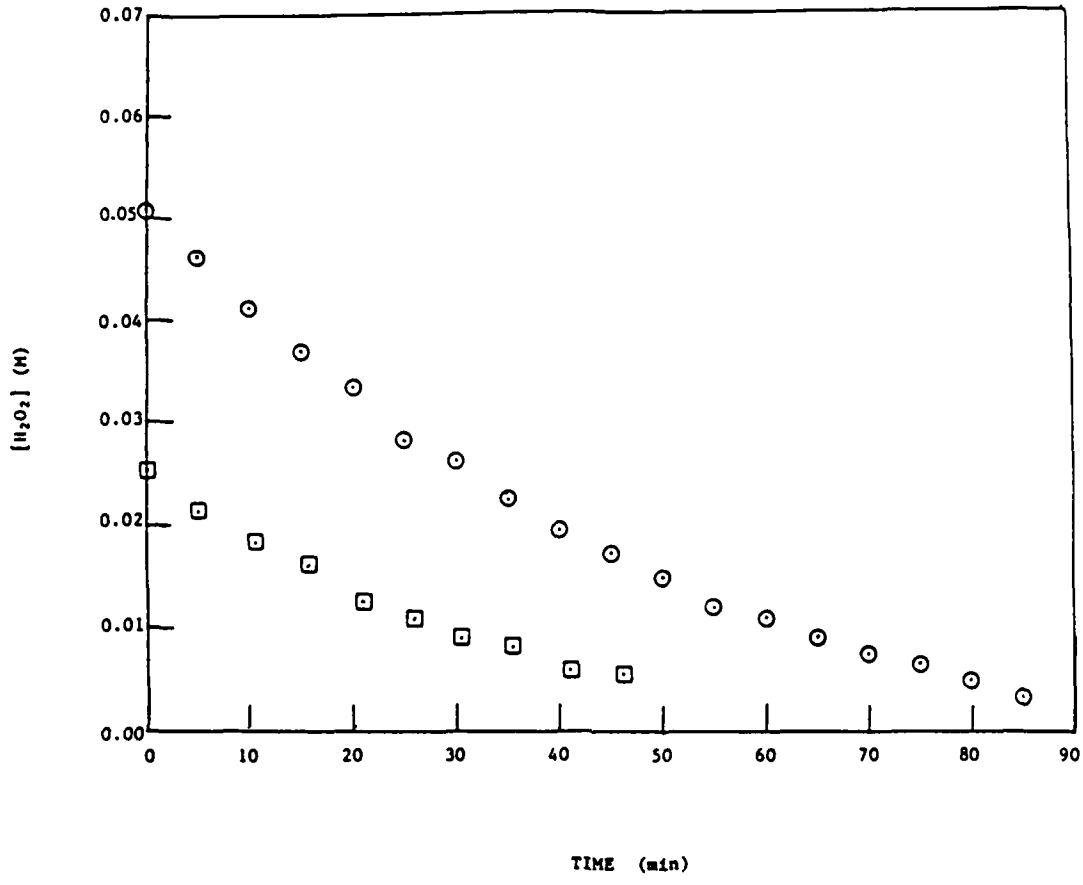

Figure 4. Concentration of Hydrogen Peroxide (H_2O_2) as a function of time under UV illumination;

$[H_2O_2]_0$ = 0.05 M (◎) and 0.025 M (⊡)

I = 1.31 W/0.2L

T_0 = 23°C

pH = 2.20

pH_f = 2.07

By applying Eq. 10 to Scheme I one can equate the concentrate of $HO_2^{\cdot}$ to H_2O_2 and $OH^{\cdot}$ according to the following relation

$$(HO_2\cdot) = \sqrt{\frac{k_2(H_2O_2)(OH\cdot)}{k_3}} \tag{11}$$

The steady state approach for $OH^{\cdot}$ gives the following equation for the $OH^{\cdot}$ concentration

$$(OH\cdot) = \frac{2\ k_1}{k_2} \tag{12}$$

which requires a value for k_1 in order to be solved. The k_1 value can be obtained by first establishing the overall rate equation for H_2O_2 removal. From Scheme I this becomes

$$\frac{-\ d(H_2O_2)}{dt} = k_1(H_2O_2) + k_2(H_2O_2)(OH\cdot) - k_3(HO_2\cdot)^2 \tag{13}$$

Substituting Eq. 11 into Eq. 13 gives

$$\frac{-\ d(H_2O_2)}{dt} = k_1(H_2O_2) \tag{14}$$

which is consistent with the first-order behavior observed in Figure 4. Integration of Eq. 14 and rearrangement yields an expression for k_1 given by the following equation

$$k_1 = \frac{1}{\Delta t} \ln \frac{(H_2O_2)}{(H_2O_2)_o} \tag{15}$$

The absolute value of k_1 is actually a function of the H_2O_2 concentration, its quantum efficiency and the light intensity.

The quantum yield for hydrogen peroxide removal can be determined once the number of photons absorbed by H_2O_2 is estimated. The relationship between the extent of absorption of radiation and the H_2O_2 concentration is given by the Beer-Lambert law:

$$I = I_o \, 10^{-\varepsilon_{H_2O_2} C_{H_2O_2}} \tag{16}$$

where I_o is the source intensity at 254 nm, I is the transmitted intensity and $\varepsilon_{H_2O_2} = 19$ and $C_{H_2O_2}$ are the molar absorbtivity and concentration of H_2O_2 respectively. Since the absorbed intensity ($I_{H_2O_2}$) is the difference between I and I_o, Eq. 16 can be rewritten in the form

$$I_{H_2O_2} = I_o \left(1-10^{-\varepsilon_{H_2O_2} C_{H_2O_2}}\right) \tag{17}$$

The initial quantum yield for H_2O_2 removal is now given by

$$\eta_{H_2O_2} = \frac{-\frac{d(H_2O_2)}{dt}}{I_{H_2O_2}} \tag{18}$$

Some kinetic parameters determined from the hydrogen peroxide decomposition data in Figure 4 are listed in Table 2.

TABLE 2. KINETIC PARAMETERS FOR H_2O_2 PHOTOLYSIS*

$[H_2O_2]$ (M)	$\frac{-d(H_2O_2)_o}{dt}$** ($M \cdot s^{-1}$)	k_1 (s^{-1})	$[OH^\cdot]$ (M)	$[HO_2^\cdot]$ (M)	$\eta_{H_2O_2}$
0.05	1.39×10^{-5}	3.8×10^{-4}	2.5×10^{-11}	6.7×10^{-6}	1.13
0.025	9.58×10^{-6}	5.6×10^{-4}	3.7×10^{-11}	5.7×10^{-6}	1.03

*$I_o = 1.39 \times 10^{-5}$ $M \cdot s^{-1}$

**Extrapolated initial linear decay.

The low values for the $[OH^\cdot]$ are indicative of the high reactivity of the hydroxyl radical in aqueous media. The estimated quantum yields are in close agreement with those reported by Dainton and Rowbottom [15].

4.2.2 TNT/H_2O_2/UV System

As a control experiment in the study of this system, TNT was first run in the presence of 0.05 M H_2O_2 without photolysis. The concentrations of TNT, H_2O_2 and total oxidants (by BKI/M method) were followed with time (Figure 5). The results show that essentially no hydrogen peroxide decomposition or TNT destruction occurred within the time frame of the experiment.

The decomposition of TNT was then carried out at the 0.4 and 0.2 mM concentrations under H_2O_2/UV conditions in an acidic environment.

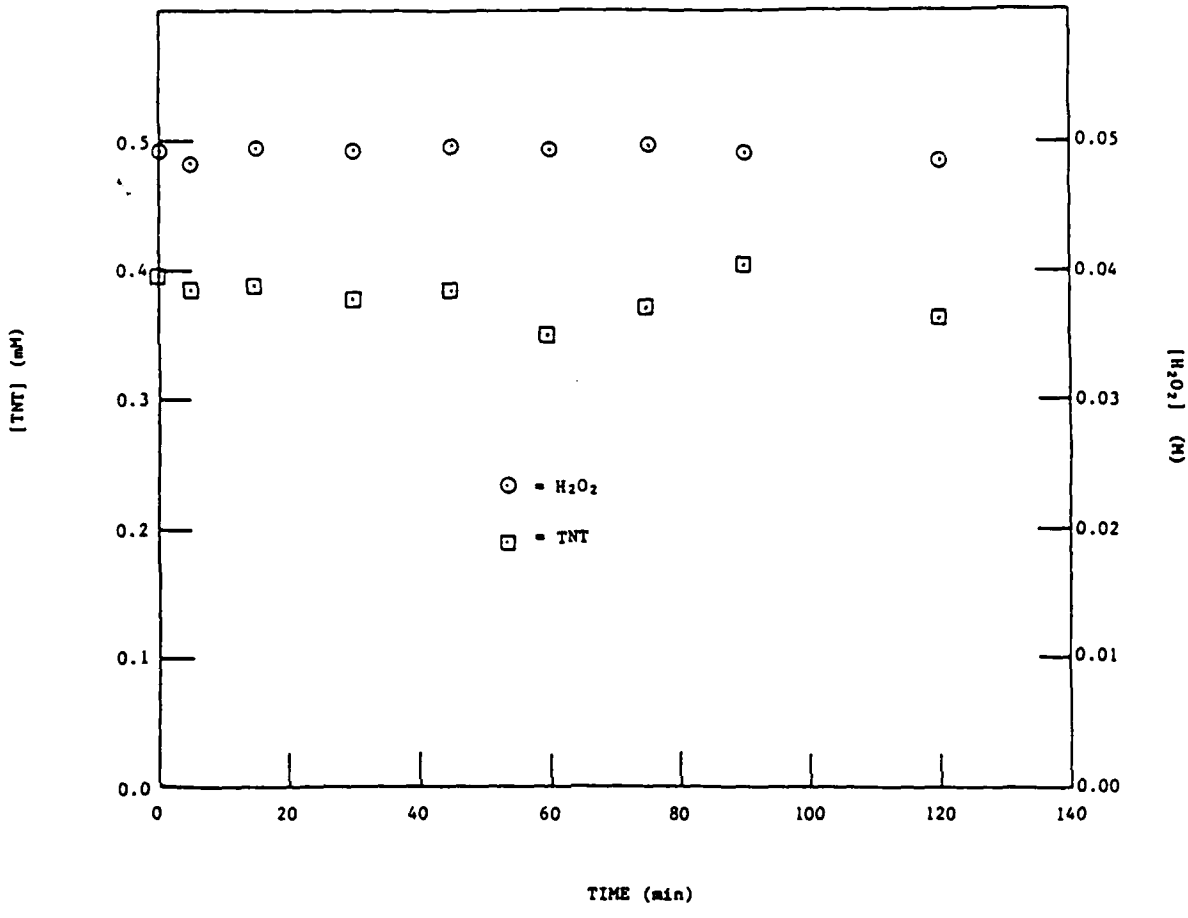

Figure 5. Concentration of 2, 4, 6-trinitrotoluene (TNT) and Hydrogen Peroxide (H_2O_2) versus time under dark conditions;

$[H_2O_2]_0$ = 0.05 M

$[TNT]_0$ = 0.4 mM

T_0 = 23°C

T_f = 23°C

pH_0 = 1.83

pH_f = 1.82

The initial hydrogen peroxide concentration in these experiments was 0.05 M and the illumination intensity at λ = 254 nm was 1.39×10^{-5} ein$\cdot s^{-1}$. Plots for the loss of TNT and H_2O_2 with time are shown in Figures 6, 7 and 8. Using the Meissenheimer complex formation between TNT and sulfite as an analytical tool, it was discovered that as the concentration of TNT decreases initially there is an increase in the concentration of trinitrobenzene. In Figures 6, 7 and 8 the TNB concentration can be seen to reach a maximum when the TNT concentration drops to approximately 25 percent of its initial value. It is obvious from these curves that the rate of TNB removal is much slower than the removal of TNT.

A possible mechanism for this system involves reactions which compete for hydroxyl radicals as in the following sequence of steps

Scheme II:

$$H_2O_2 \xrightarrow{k_1} 2\ (\cdot OH) \tag{19}$$

$$TNT + \cdot OH \xrightarrow{k_{TNT}} (TNT)_{ox} \tag{20}$$

$$TNB + \cdot OH \xrightarrow{k_{TNB}} (TNB)_{ox} \tag{21}$$

$$H_2O_2 + \cdot OH \xrightarrow{k_2} HO_2\cdot + H_2O \tag{22}$$

$$2\ (HO_2\cdot) \xrightarrow{k_3} H_2O_2 + O_2 \tag{23}$$

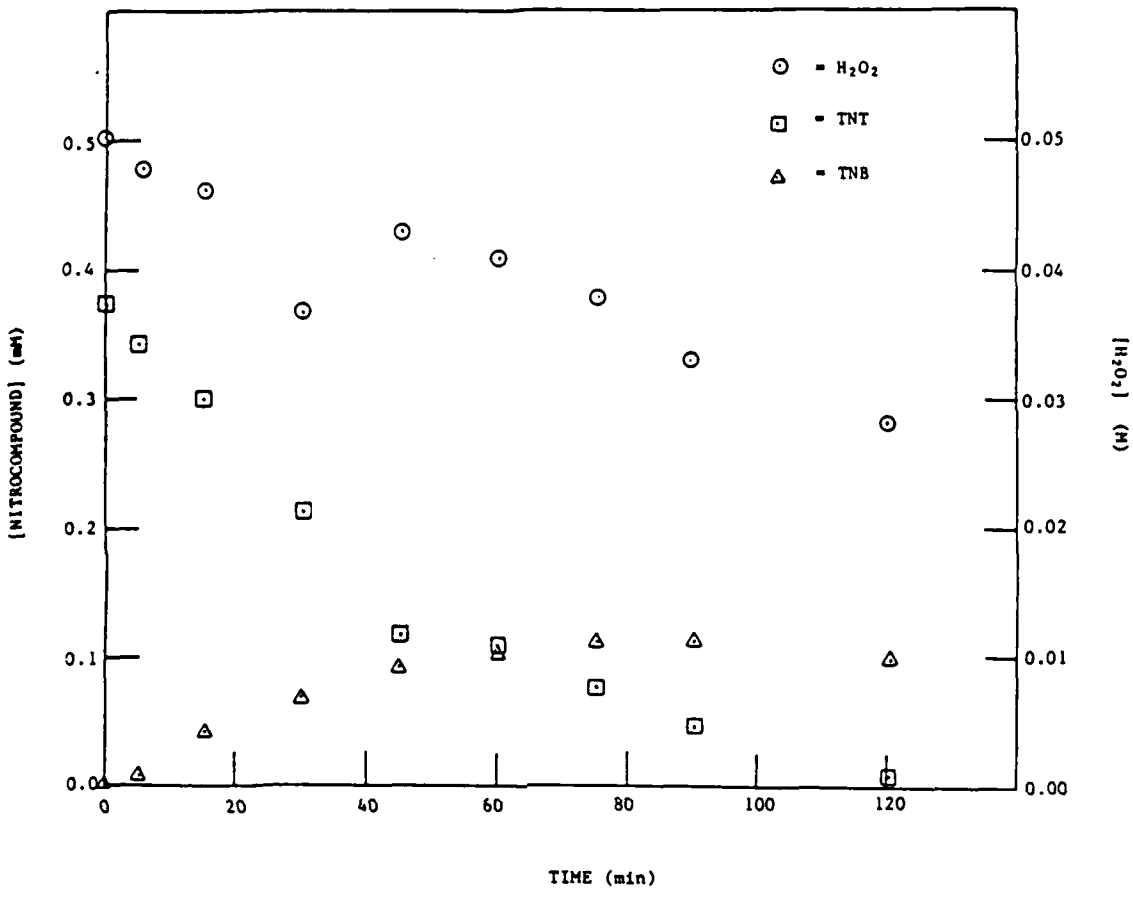

Figure 6. Concentration of H_2O_2, TNT, and 1, 3, 5-trinitrobenzene (TNB) versus time in the presence of ultraviolet light;

$[TNT]_0$ = 0.4 mM

$[H_2O_2]_0$ = 0.05 M

I = 1.31 W/0.2L

T_0 = 23°C

T_f = 33°C

pH_0 = 1.90

pH_f = 1.77

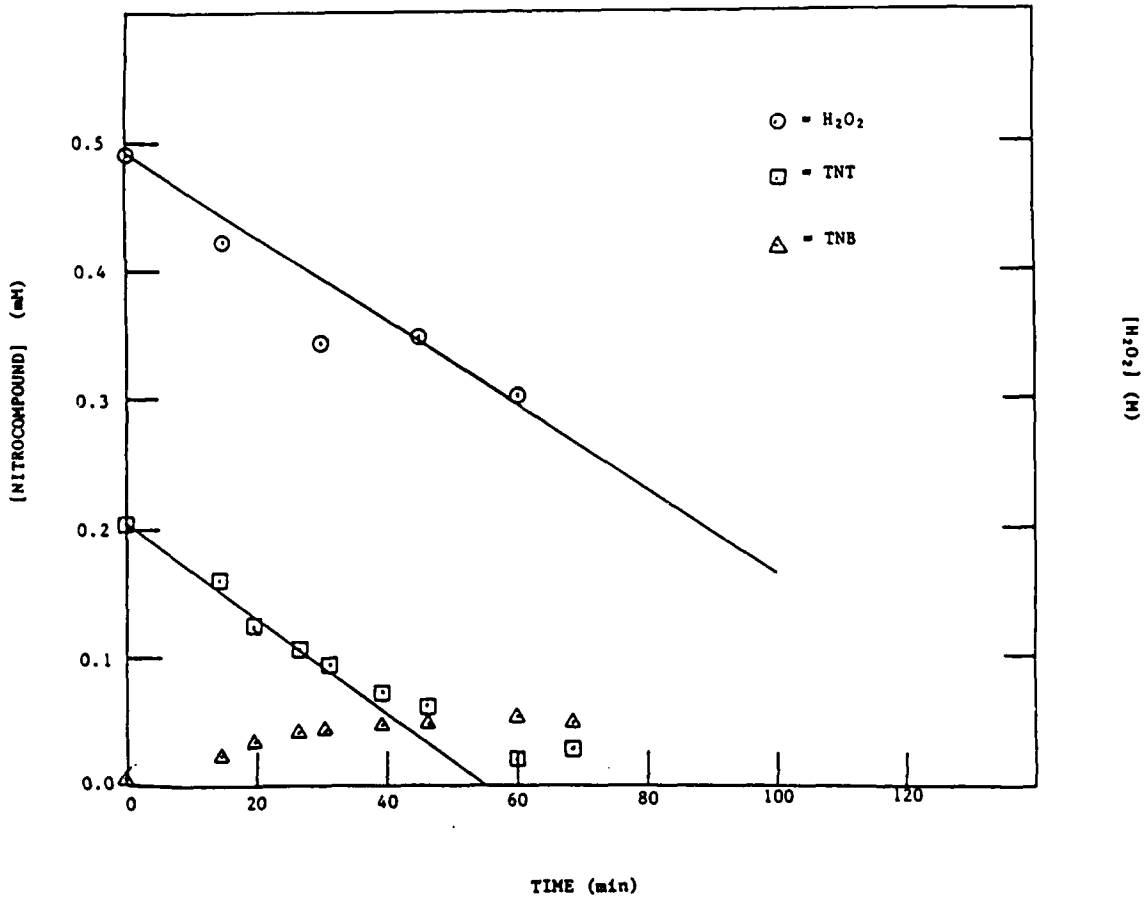

Figure 7. Concentration of H_2O_2, TNT, and TNB versus time in the presence of UV light;

$[TNT]_0$ = 0.2 mM

$[H_2O_2]_0$ = 0.05 M

I = 1.31 W/0.2L

$[TNB]_0$ = 0.0 mM

T_0 = 23°C

T_f = 33°C

pH_0 = 1.87

pH_f = 1.73

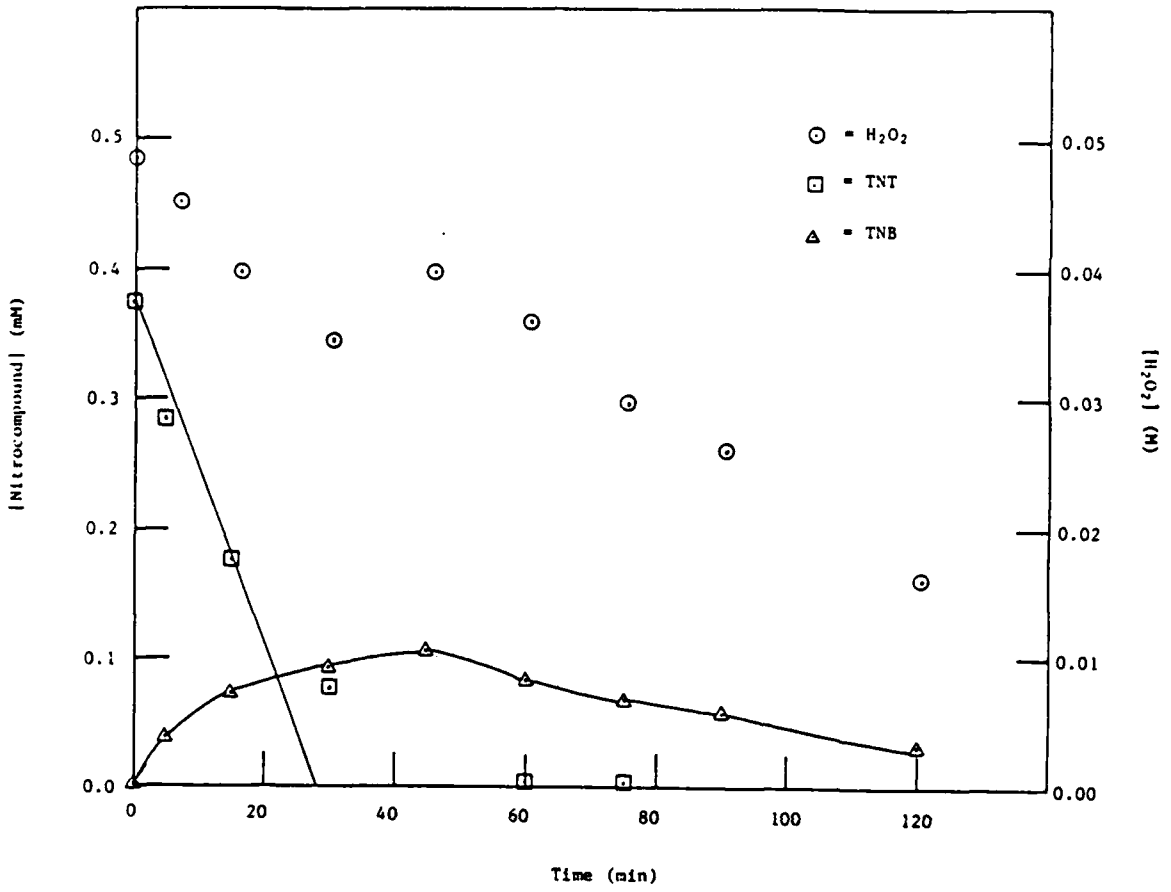

Figure 8. Concentration of H_2O_2, TNT, and TNB as a function of time with UV light at neutral pH.

$[TNT]_0$ = 0.4 mM
$[H_2O_2]_0$ = 0.05 M
I = 1.31 W/0.2L
$[TNB]_0$ = 0.0 mM
T_0 = 23°C
T_f = 34°C
pH_0 = 5.43
pH_f = 2.95

In this mechanism, the low concentration of TNB initially and at short time should make reaction 21 insignificant in terms of 'OH consumption by TNB. The overall analysis of this scheme to a final rate equation is done in a quite similar manner as presented in 4.2.1 for the H_2O_2/UV system, except now we must take into account the organic constituents, in terms of both their direct interaction with the radicals and the interactions with the incident photons. If we assume that the TNB reaction is negligible at least initially, and apply the steady-state approximation for ('OH) and (HO_2'), then the concentrations of these species are given by

$$(\cdot OH) = \frac{2\ k_1(H_2O_2)}{k_{TNT}(TNT) + k_2(H_2O_2)} \tag{24}$$

$$(HO_2\cdot) = \left[\frac{2\ k_2(H_2O_2)(\cdot OH)}{k_3}\right] \tag{25}$$

The rate of TNT removal is

$$\frac{d(TNT)}{dt} = -\ k_{TNT}(TNT)(\cdot OH)$$

$$= \frac{-\ 2\ k_1\ k_{TNT}(H_2O_2)(TNT)}{k_{TNT}(TNT) + k_2(H_2O_2)} \tag{26}$$

Since the product between k_1 and (H_2O_2) extrapolates back to the removal rate for hydrogen peroxide (see discussion of Eq. 14), Eq. 26 can be rewritten as

$$\frac{d(TNT)}{dt} = \frac{2\ k_{TNT}(TNT)\ \frac{d(H_2O_2)}{dt}}{k_{TNT}(TNT) + k_2(H_2O_2)} \tag{27}$$

or

$$\frac{1}{\frac{d(TNT)}{dt}} = \frac{1}{2\ \frac{d(H_2O_2)}{dt}} \left[1 + \frac{k_2(H_2O_2)}{k_{TNT}(TNT)}\right] \tag{28}$$

The rate of loss of TNT and H_2O_2 can be obtained directly from the initial experimental removal data.

The resulting equations relating the loss of TNT to the loss of H_2O_2 can also take into account any additional reactions that compete with TNT for hydroxyl radical by expanding the general form of Eq. 28, giving

$$\frac{d(TNT)}{dt} = 2\ k_{TNT}(TNT)\ \frac{d(H_2O_2)}{dt} \left[\sum_i k_i(i)\right]^{-1} \tag{29}$$

where there are now i competing reactions. Similarly the loss of any i-th component can be described by substituting its parameters in place of those for TNT in Eq. 29.

The light absorbed by hydrogen peroxide in the presence of other absorbing constituents in aqueous solutions can be determined using Beer-Lambert's law for which the general formulation is

$$I_{H_2O_2} = \frac{(H_2O_2)\varepsilon_{H_2O_2}}{(H_2O_2)\varepsilon_{H_2O_2} + \sum_i (i)\varepsilon_i} \left(1-10^{-(C_{H_2O_2}\ \varepsilon_{H_2O_2} + C_{TNT}\ \varepsilon_{TNT})}\right) I_o \qquad (30)$$

where $I_{H_2O_2}$ is the number of quanta absorbed by H_2O_2 in the solution in einsteins - sec^{-1}, ε represents the molar extinction coefficient of the solute indicated by the subscript and I_o is the incident light flux at the given wavelength. The values of the extinction coefficients at λ = 254 nm are ε_{TNT} = 3300 and $\varepsilon_{H_2O_2}$ = 19 [6, 10].

The quantum yield for the destruction of TNT can be calculated using the following equation

$$\eta_{TNT} = \frac{-\frac{d(TNT)}{dt}}{I_{H_2O_2}} \qquad (31)$$

which represents the rate of TNT removal to the fraction of photons absorbed by the hydrogen peroxide as in Eq. 18. With an equation similar to that above the quantum yield for H_2O_2 or any other constituent can also be identified and used for rate comparisons. According to Scheme II in the absence of TNB, the experimental and kinetic parameters for the destruction of TNT and the H_2O_2/UV system are given in Table 3.

Certain trends can be developed from the tabulated data. For example, as predicted, the number of photons absorbed by H_2O_2 decreases as the concentration of other species that absorb at 254 nm increases. The higher TNT concentration also results in a larger quantum yield

TABLE 3. LIST OF EXPERIMENTAL AND KINETIC PARAMETERS FOR H_2O_2/UV AND TNT/H_2O_2/UV EXPERIMENTS

Conditions	pH* (pH_o/pH_f)	$[H_2O_2]_o$ (M)	$[TNT]_o$ (mM)	$\frac{-d[H_2O_2]_o}{dt}$ ($M \cdot s^{-1}$)	$\frac{-d[TNT]_o}{dt}$ ($M \cdot s^{-1}$)	$I^{\circ}_{H_2O_2}$**,a ($Ein \cdot s^{-1}$)	$\eta_{H_2O_2}$	η_{TNT} b	k_1 (s^{-1})	k_{TNT} ($M^{-1} \cdot s^{-1}$)	$[^{\cdot}OH]$ (M)	$[HO_2^{\cdot}]$ (M)
H_2O_2/UV	1.9	0.05	-	1.1×10^{-5}	--	1.2×10^{-5}	0.94	--	3.5×10^{-4}	--	2.3×10^{-11}	6.4×10^{-6}
H_2O_2/UV/TNT	1.9/1.77	0.05	0.4	2.4×10^{-6}	9.1×10^{-8}	5.8×10^{-6}	0.42	1.6×10^{-2}	5.8×10^{-5}	7.1×10^{7}	3.8×10^{-12}	3.6×10^{-6}
H_2O_2/UV/TNT	1.87/1.73	0.05	0.2	5.3×10^{-6}	6.0×10^{-8}	7.4×10^{-6}	0.71	8.1×10^{-3}	1.3×10^{-4}	4.3×10^{7}	9.1×10^{-12}	5.6×10^{-6}
H_2O_2/UV/TNT	5.4/2.9	0.05	0.4	8.3×10^{-6}	2.3×10^{-7}	5.8×10^{-6}	1.43	4.0×10^{-2}	5.3×10^{-4}	5.2×10^{7}	3.5×10^{-4}	1.1×10^{-5}

*pH initial (o) and final (f)

**$I_o = 1.39 \times 10^{-5}$ $Ein \cdot s^{-1}$

a$\epsilon_{H_2O_2} = 19$, $\epsilon_{TNT} = 3300$

b$\eta_{TNT} = \frac{\frac{-d[TNT]_o}{dt}}{I^{\circ}_{H_2O_2}}$

because as the concentration of TNT decreases, the self scavenging of $^{\cdot}OH$ by H_2O_2 increases. This is further substantiated by the peroxide quantum yield trend. The low concentration of $^{\cdot}OH$ is indicative of their short lifetimes and high reactivity as compared to the hydroperoxy radical present in micromolar concentrations. The system having an initial higher pH showed both a larger quantum yield for H_2O_2 and TNT, perhaps due to a decreased stability of the H_2O_2. It is also apparent that the solution is acidified during the course of the experiment. However, more importantly these experiments suggested that TNB removal is the bottleneck in the destruction of polynitrated benzenes. This is in agreement with the O_3/UV results and those of Andrews and Osmon [16]. For this reason, the efficacy and kinetics of the TNB/H_2O_2/Uv system and effects of varying the H_2O_2/UV experimental parameters were investigated more extensively.

4.2.3 TNB/H_2O_2/UV System

This system was examined under a number of different environmental conditions including various initial TNB concentrations, light intensities, temperature and pH. A number of experiments having different environments were done specifically to follow the course of the TNB destruction and for intermediate product identification. The analytical procedures included GC/MS, TOC, ion chromatography for nitrate and direct aqueous injection GC. All TNB experiments had an initial TNB concentration of 0.2 mM.

The system tested by GC/MS initially contained 0.05 M H_2O_2 and was photolyzed with a UV intensity of 1.39×10^{-5} ein$^{\cdot}s^{-1}$. During the run, solution samples were taken at 70 minutes at which time 0.113 mM of TNB remained and at 150 minutes where only 0.014 mM of TNB was detected spectrophotometrically. These samples along with a zero time and distilled water (solvent blank) were extracted using ether and concentrated. Two different chromatographic procedures were used to analyze the

extracts. One system consisted of a column fitted with packings having a liquid phase of three percent SP 2250 supported on Supelcopak. This system is designed to isolate neutral and basic organic products. The other system utilized a column packed with a liquid phase of three percent SP 1240 DA on Supelcopak. This phase is usually used for the analysis of nitrated and chlorinated phenols and other polar systems. The diazomethane derivatization procedure was conducted to convert any carboxylic acids and phenolics, that are often intermediate products in the oxidation of organics, into methyl esters which can then be chromatographed on the nonpolar column.

All the samples except the blank indicated the presence of TNB in amounts consistent with that measured above. The GC/MS results also showed the presence of peroxides from the ether used to extract the samples and other general contaminants. The methyl esters of carboxylic acids and phenolics were not found nor were any nitrophenols detected.

The results of the total organic carbon analyses for the different systems sampled are given in Table 4. The zero time base results corresponds precisely with the theoretical 14.4 mg/L for 0.2 mM TNB. The TOC values in general indicate that considerable organic carbon is still present even though TNB has almost been completely destroyed. The removal of TOC is also not linear with time; compare the TOC values at 70 and 150 minutes in experiments 2 and 3 in Table 4. The rate at which the TOC in solution dropped also decreases with lower initial H_2O_2 concentration and even more so when the light intensity was cut by 75 percent. These last two conditions will be discussed more thoroughly later in this section.

Although the GC/MS analyses did not identify the presence of any carboxylic acids, it is highly likely that low molecular weight acids are stable oxidative reaction products. The same system used for

TABLE 4. TOC ANALYTICAL RESULTS FOR H_2O_2/UV/TNB SYSTEMS

Experiment	TNB Conc. (mM)	H_2O_2 Conc. (M)	I_o^* ($ein \cdot s^{-1}$)	Sampling Time (min)	TOC (mg/L)
1	0.1	-	-	0	7.2
2	0.2	0.05	1.39×10^{-5}	70	13
3	0.2	0.05	1.39×10^{-5}	150	6
4	0.2	0.01	1.39×10^{-5}	120	8
5	0.2	0.05	3.28×10^{-6}	120	12

*λ = 254 nm.

the GC/MS and TOC (Experiment 2 and 3) analyses were rerun for 120 minutes. Samples were then subjected to benzyl bromide derivatization and subsequent GC analysis. This analysis procedure revealed that the main reaction products were formic and acetic acid at a concentration of 0.260 mM and 0.080 mM respectively. Taking into account that 0.034 mM of TNB was also present in this 120 minute sample the estimated TOC level is 7.5 mg/L in good agreement with the independent analysis. Thus, the GC results suggest that these small acid molecules could account for the TOC remaining after complete loss of TNB.

Nitrate analysis was performed on samples taken during the course of the H_2O_2/UV removal of TNB. The initial TNB concentration was 0.2 mM and the initial H_2O_2 concentration was 0.05 M. The ion chromatographic results are listed in Table 5. A spiked control sample was correctly analyzed at the 17 mg/L level. These data show that, at least initially (up to 30 min), the nitrate appearance in solution follows the destruction of TNB. Since the GC/MS results did not show any nitrophenolic products, either ring cleavage must occur or unstable ring intermediates must be formed which quickly react with additional radical species to generate smaller products that were undetectable by GC/MS. In the latter stages of the run, the nitrate concentration appears to reach a steady state and even decrease somewhat. Since no organo-nitro products were detected, the nitrate may be undergoing photolysis and lost via some gaseous product.

Kinetic and efficiency information was obtained by evaluating and comparing the loss rate data from a series of H_2O_2/UV experiments using TNB as the substrate. The concentration vs. time plots of TNB and H_2O_2 for the systems examined are presented in Appendix A. The same mechanistic approach as was taken in the discussion of the TNT/H_2O_2/UV system was also adopted for evaluating the TNB system. A list of some of the experimental conditions and calculated kinetic parameters are given in Table 6.

TABLE 5. NITRATE ANALYTICAL DATA FOR $H_2O_2/UV^*/TNB$

Time (min)	TNB Conc. (mM)	NO_3^- (mg/L)
0	0.2	< 0.5
30	0.151	7.5
60	0.116	3.1
70	0.113	5.5
90	0.070	6.3
120	0.037	6.3

*$I_o = 1.39 \times 10^{-5}$ ein·s^{-1}.

TABLE 6. LIST OF EXPERIMENTAL AND KINETIC PARAMETERS FOR TNB/H_2O_2/UV EXPERIMENTS

Figure No.	pH* (pH_o/pH_f)	$[H_2O_2]_o$ (M)	$[TNB]_o$ (mM)	$\frac{-d[H_2O_2]_o}{dt}$ ($M \cdot s^{-1}$)	$\frac{-d[TNB]_o}{dt}$ ($M \cdot s^{-1}$)	$I^{\circ}_{H_2O_2}$ **,a ($Ein \cdot s^{-1}$)	$\eta_{H_2O_2}$ b	η_{TNB} b	$k_{H_2O_2}$ (s^{-1})	k_{TNB} ($M^{-1} \cdot s^{-1}$)	$[^{\cdot}OH]$ (M)	$[HO_2^{\cdot}]$ (M)
1	1.9	0.05	-	1.1×10^{-5}	--	1.2×10^{-5}	0.94	--	3.5×10^{-4}	--	2.3×10^{-11}	6.4×10^{-6}
B-1	1.84/1.74	0.05	0.2	4.0×10^{-6}	2.1×10^{-8}	8.2×10^{-6}	0.44	2.6×10^{-3}	1.1×10^{-4}	2×10^{7}	7.3×10^{-17}	5.0×10^{-6}
B-2	1.86/1.77	0.025	0.2	2.3×10^{-6}	2.3×10^{-8}	5.6×10^{-6}	0.41	4.1×10^{-3}	1.2×10^{-4}	1.8×10^{7}	8.0×10^{-12}	3.7×10^{-6}
B-3	1.82/1.74	0.01	0.2	1.0×10^{-6}	2.4×10^{-8}	2.8×10^{-6}	0.36	8.6×10^{-3}	1.4×10^{-4}	1.8×10^{7}	9.2×10^{-12}	2.5×10^{-6}
B-4	1.87/1.79	0.05	0.2	2.1×10^{-6}	1.2×10^{-8}	3.2×10^{-6} c	0.64	3.8×10^{-3}	5.4×10^{-5}	2.2×10^{7}	3.6×10^{-17}	3.5×10^{-6}
B-5	1.79/1.70	0.05	0.2	1.4×10^{-6}	3.1×10^{-9}	1.0×10^{-6} d	1.41	3.1×10^{-3}	1.7×10^{-5}	8.1×10^{6}	1.1×10^{-12}	1.9×10^{-6}
B-6	5.6/3.2	0.05	0.2	3.7×10^{-6}	1.8×10^{-8}	8.2×10^{-6}	0.45	2.3×10^{-3}	1.0×10^{-4}	1.9×10^{7}	6.8×10^{-17}	4.9×10^{-6}
B-7	1.85/1.72	0.05	0.2	2.9×10^{-6}	1.3×10^{-8}	8.2×10^{-6}	0.35	1.7×10^{-3}	7.6×10^{-5}	1.8×10^{7}	5.0×10^{-11}	1.3×10^{-5}

*pH initial (o) and final (f)

**$I_o = 1.39 \times 10^{-5}$ $Ein \cdot s^{-1}$

a$\epsilon_{H_2O_2} = 19$, $\epsilon_{TNT} = 3300$, $\epsilon_{TNB} = 3000$

b$\eta = \frac{\frac{-d(x)_o}{dt}}{I^{\circ}_{H_2O_2}}$

c$I_o = 5.5 \times 10^{-6}$ $Ein \cdot s^{-1}$

d$I_o = 1.7 \times 10^{-6}$ $Ein \cdot s^{-1}$

The average rate constant for the destruction of TNB via reaction with $^{\cdot}OH$ is $1.6 \times 10^{7}\ M^{-1} \cdot s^{-1}$ as compared to the TNT rate constant $k_{TNT}^{avg.} = 5.5 \times 10^{7}\ M \cdot s^{-1}$ from Table 3. In the case of TNT removal, it has been demonstrated that the major reaction product is TNB but, for TNB oxidation we will assume for the most part that ring cleavage occurs. A more detailed examination of reaction products will be presented below. The rate constant was calculated on the basis that the reaction requires only one hydroxyl radical per TNB molecule consumed. If more than one $^{\cdot}OH$ is consumed in the RDS (See Eq. 21) the effect on the rate constant would be to double its value per $^{\cdot}OH$ needed. In general, the comparison of rate constants for TNT and TNB are consistent with the removal behavior observed under H_2O_2/UV conditions where the loss of TNB determines the overall rate of polynitrated benzene destruction.

The results in Table 6 show that decreasing the initial H_2O_2 concentration from 0.05 M to 0.01 M causes a reduced quantum yield for H_2O_2 removal as would be expected but, concurrently also increases the quantum yield for TNB loss (Figures A-1, A-2 and A-3). This fact indicates the importance of the concentration of H_2O_2 on the efficient removal of species that must compete for $^{\cdot}OH$. Thus, depending on the rate constants of other solution constituents and their concentration, in some cases hydrogen peroxide itself can dominate the consumption of $^{\cdot}OH$. On the other hand, the low molar extinction coefficient of H_2O_2 requires as high a concentration as possible in order to obtain maximum light absorption.

The effect of the incident photon intensity on the peroxide removal is numerically illustrated for the results of Figures A-1, A-4 and A-5. As the UV intensity decreases, the quantum yield for H_2O_2 absorption increases with, however, no influence on the yield for TNB removal. Thus, the light intensity has no effect on the actual number of $^{\cdot}OH$ molecules needed to oxidize TNB but does directly effect the overall TNB removal rate, -d(TNB)/dt.

The experiment involving the higher pH condition (pH_o = 6.0) did not show an increase in substrate removal rate and quantum yield for TNB as it did for TNT. Although this might suggest some pH dependency on the demethylation of TNT under H_2O_2 photolysis, a more detailed explanation is not possible from the pH data on hand. Fundamental studies at controlled pH are difficult in such a system since $^{\cdot}OH$ reacts with many species commonly used as pH buffers. The run done at higher temperature (70°C) revealed no advantage over the ambient system, and in fact showed a slight decrease in the TNB removal rate.

As an independent check on the mechanism and rate constant determined for TNB removal, additional competition experiments were done. To obtain baseline parameters for competing species, acetic acid at the 5.0 mM level was first run with 0.05 M H_2O_2 and UV illumination (I_o = 1.39 x 10^{-5} Ein·s^{-1} and pH_o = 3.54). This system is also of interest since small carboxylic acids are products of long term photo-oxidation of TNB. The decomposition plots against time are shown in Figure 9 for both acetate (Ac^-) and H_2O_2. The basic mechanism for this system is assumed to be similar to those discussed above for other H_2O_2/UV cases and is given as

$$H_2O_2 \xrightarrow{k_1} 2\ (\cdot OH) \tag{32}$$

$$Ac^- + \cdot OH \xrightarrow{k_{Ac^-}} (Ac^-)_{ox} \tag{33}$$

$$H_2O_2 + \cdot OH \xrightarrow{k_2} HO_2\cdot + H_2O \tag{34}$$

$$2\ (HO_2\cdot) \xrightarrow{k_3} H_2O_2 + O_2 \tag{35}$$

where Eq. (33) represents the oxidation of acetate and $(Ac^-)_{ox}$ the products of that reastion.

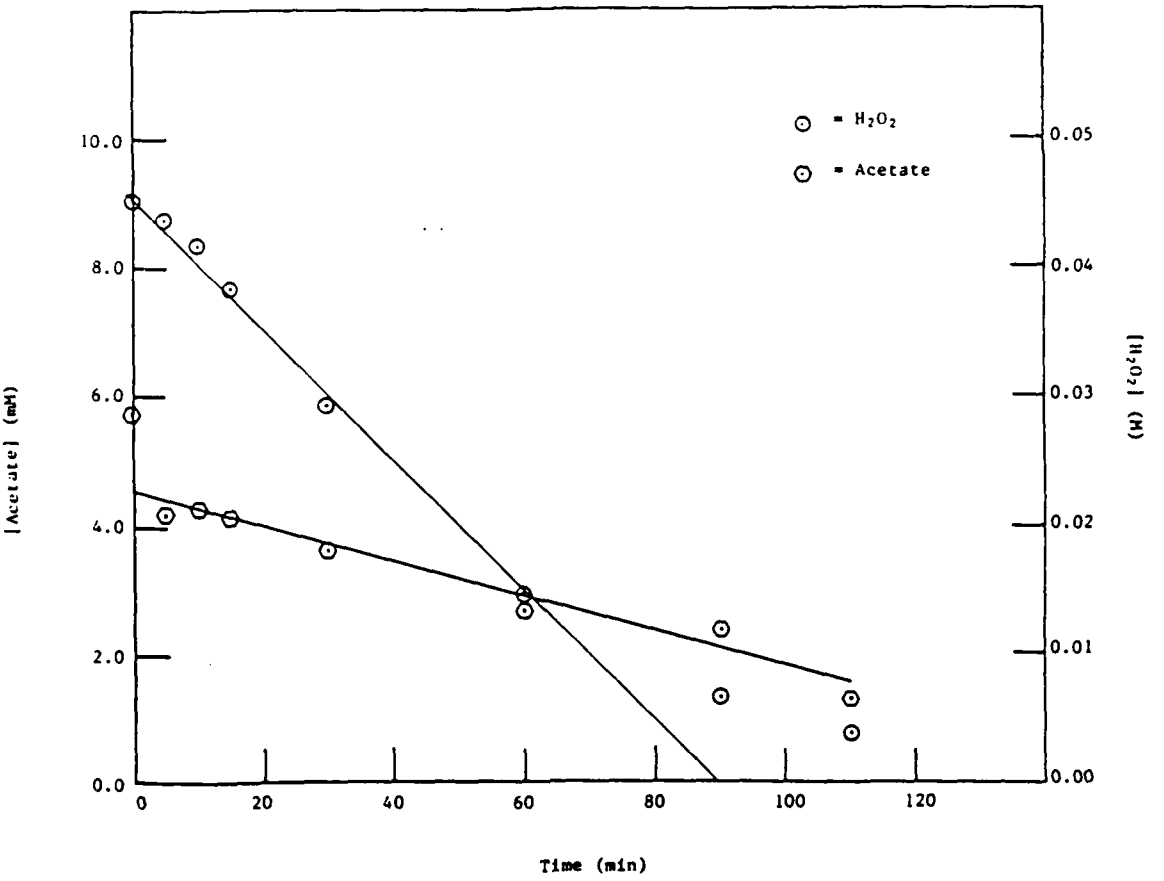

Figure 9. Concentration of Acetate and H_2O_2 versus time, with photolysis.

$[Acetate]_0$ = 5.0 mM

$[H_2O_2]_0$ = 0.05 M

I = 1.31 W/0.2L

T_0 = 23°C

T_f = 33°C

pH_0 = 3.67

pH_f = 3.51

The rate constant for acetate can then be related to the loss of H_2O_2 and acetate according to the following equation

$$k_{Ac^-} = \frac{k_2(H_2O_2)}{(Ac^-)\left[\frac{2\ d(H_2O_2)}{d(Ac^-)} - 1\right]} \qquad (36)$$

Using the initial extrapolated $-d(H_2O_2)/dt = 8.4 \times 10^{-6}\ M \cdot s^{-1}$ and $-d(Ac^-)/dt = 4.5 \times 10^{-7}\ M \cdot s^{-1}$ the calculated k_{Ac^-} was found to be $\sim 8.2 \times 10^{6}\ M^{-1} \cdot s^{-1}$.

The following experiment was carried out as just described except 0.2 mM TNB was present also. From the removal plots in Figure 10 the rates for H_2O_2 and TNB were estimated to be $6.6 \times 10^{-6}\ M \cdot s^{-1}$ and $1.89 \times 10^{-8}\ M \cdot s^{-1}$ respectively. Using a competition mechanism, the rate constant for TNB was determined from

$$k_{TNB} = \frac{k_2(H_2O_2) + k_{Ac^-}(Ac^-)}{(TNB)\left[\frac{2\ d(H_2O_2)}{d(TNB)} - 1\right]} \qquad (37)$$

to be $k_{TNB} = 1.1 \times 10^{7}\ M^{-1} \cdot s^{-1}$. This value for TNB is consistent with the average determined using the hydroxyl radical competition mechanism for the initial $TNB/H_2O_2/UV$ system examined.

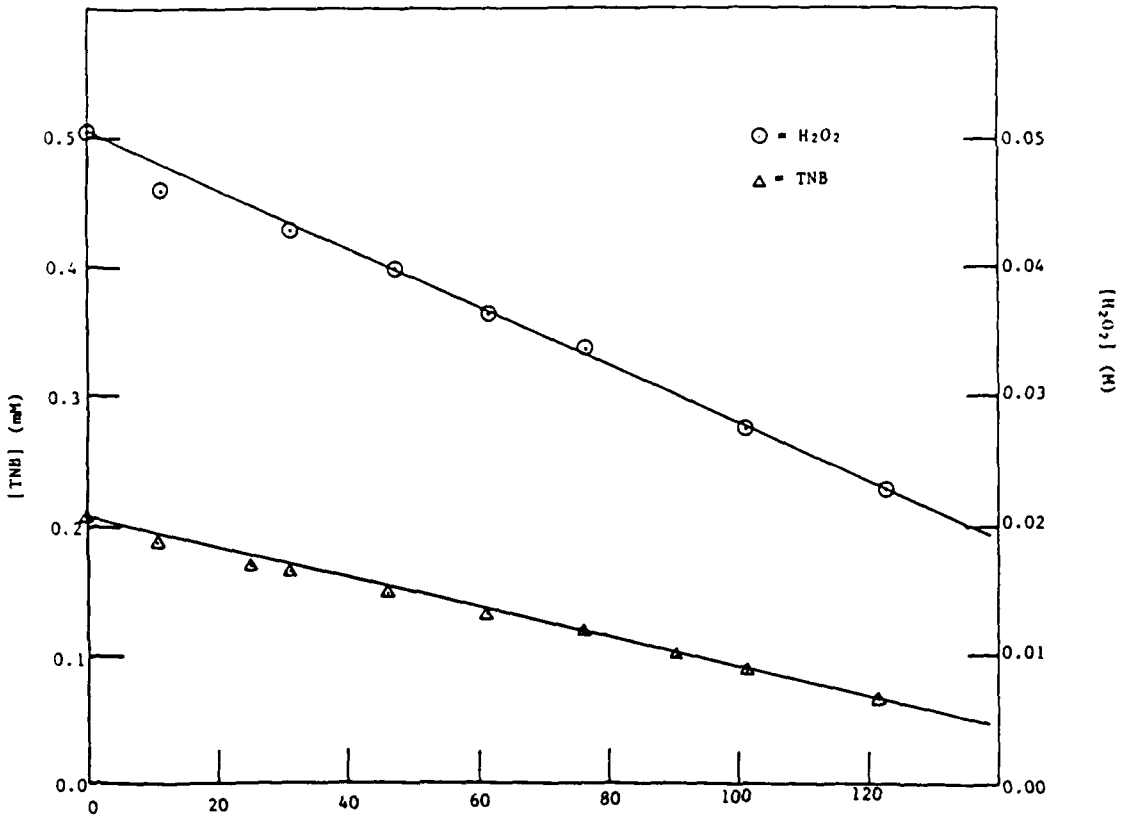

Figure 10. Concentration of TNB and H_2O_2 versus time with photolysis and in the presence of Acetic Acid.

$[TNB]_0$ = 0.2 mM
$[H_2O_2]_0$ = 0.05 M
I = 1.31 W/0.2L
$[Acetic\ Acid]_0$ = 5.0 mM
T_0 = 23°C
T_f = 34°C
pH_0 = 3.54
pH_f = 3.10

4.3 Aqueous Ozonation Systems

The oxidation strength of ozone in water is primarily determined by the rate at which ozone is decomposed into radical intermediates (vide supra). The ozonation potential increases with pH as a result of decomposition initiated by hydroxide ions. Ultraviolet radiation can also be used to initiate ozone decay. The photochemistry of O_3 in water is quite similar to that in the gas phase, however the large excess of H_2O molecules can quench product intermediates.

When ozone is decomposed in aqueous solutions the effective quantity of hydroxyl radicals available for the reaction with a substrate (S) is the product of the quantity of hydroxyl radicals generated and the relative rate with which they can react with S as compared to other possible reactions (n). The rate (R) of $^{\cdot}OH$ consumption is then given as follows

$$\Delta O_3 \longrightarrow \phi_{\cdot OH} \begin{cases} +S & R = k[S][\cdot OH] \\ +\Sigma n_i & R = [\Sigma(k_i\{n_i\})][\cdot OH] \end{cases} \qquad (38)$$

where

ΔO_3 = change in $[O_3]$ due to decay

$\phi_{\cdot OH}$ = yield of $^{\cdot}OH$ formation

k = second order reaction rate constant for $^{\cdot}OH$

$\Sigma k_i[n_i]$ = rate of $^{\cdot}OH$ consumed by all side processes.

The reaction involving S will only consume a fraction of the total $^{\cdot}OH$ yield, represented by $\phi_{\cdot OH}$. The expression for the loss of S is

$$\frac{-d[S]}{dt} = \phi_{\cdot OH}\, \phi'_{\cdot OH} \left(\frac{d[\Delta O_3]}{dt}\right) k[S]\, (\Sigma[k_i\{n_i\}])^{-1} \qquad (39)$$

and for $k[S] << \Sigma k_i[n_i]$, integration gives

$$\ln \frac{[S_o]}{[S_f]} = \phi_{\cdot OH}\, \phi'_{\cdot OH}\, (\Delta O_3)\, k(\Sigma[k_i\{n_i\}])^{-1} \qquad (40)$$

where $[S_o]$ and $[S_f]$ represent the initial and final substrate concentrations respectively. From the above equation one finds that the amount of ozone that must decompose decreases linearly with respect to the rate constant for the ozone/substrate reaction, while on the other hand the rate of ozone decay must increase linearly in relation to the rate of the scavenging of $^{\cdot}OH$ via side reactions. This model agrees quite well with the known rate constants for many $^{\cdot}OH$ radical-substrate systems [17].

4.3.1 2,4,6-Trinitrotoluene (TNT)/O_3/UV System

The destruction of 0.4 mM TNT level was carried out using 0.5 percent O_3 at a flow rate of 500 mL/min in the presence of UV light ($I_o^{254} = 1.39 \times 10^{-5}$ ein$\cdot s^{-1}$). The test solution contained 0.01 M H_2SO_4 (pH $\sim$ 1.8). The concentration of TNT during the course of this experiment was followed by measuring the absorbance of the TNT-sulfite Meisenheimer complex. The experimental data plotted in Figure 11 show that

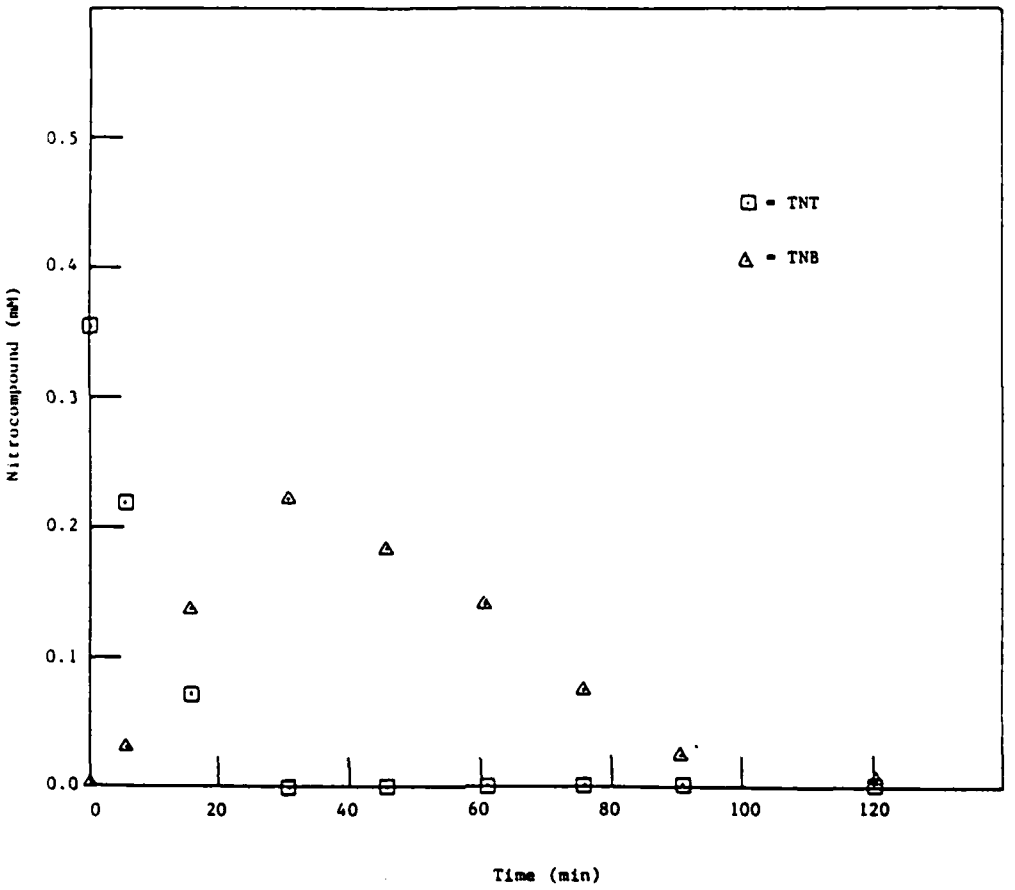

Figure 11. Concentration of TNT and TNB versus time with Ozone and UV light.

$[TNT]_0$ = 0.4 mM

$[TNB]_0$ = 0.0 mM

O_3 Dose rate = 6.6×10^{-6} M•s^{-1}

I = 1.31 W/0.2L

T_0 = 23°C

T_f = 32°C

pH_0 = 1.91

pH_f = 1.76

the half-life of TNT under these conditions is between 5 and 10 minutes. The major TNT oxidation product is 1,3,5-trinitrobenzene (TNB). The TNB concentration vs. time in this case is also shown in Figure 11 as determined by absorbance measurements of the TNB-Meisenheimer complex. These results indicate that at this rate of O_3 consumption the overall yield for TNT oxidation is well above 0.6. Another important fact shown by this experiment is that TNT can be destroyed relatively easily by O_3/UV but the bottleneck in removing the polynitro-substituted benzene components is TNB. For this reason, the remaining discussion of the O_3/UV system will focus on the destruction of trinitrobenzene in solution. A more detailed discussion of TNB oxidation reactions involving radical intermediates is presented in the next section.

4.3.2 TNB/O_3 System in the Dark

An experiment was done in which a 0.2 mM TNB solution (0.01 M H_2SO_4) was ozonated without UV illumination at a dose rate of 0.58 percent O_3 at 500 mL/min (19 mg $O_3 \cdot L^{-1} \cdot min^{-1}$) and the concentration of TNB followed with time. The resulting destruction plot is given in Figure 12. The linear removal rate is 2.2×10^{-8} $M \cdot s^{-1}$. The amount of O_3 used, taken as the difference between the dose rate and escape rate of unreacted O_3 in the exit gas, was 1.9 mg $O_3 \cdot L^{-1} \cdot min^{-1}$ or 6.6×10^{-7} $M \cdot s^{-1}$. The efficiency for TNB removal by O_3 is calculated to be $\sim$ 0.033 or in other words the destruction of one molecule of TNB requires about 30 molecules of O_3. The overall efficiency relative to the total O_3 input to the system is 0.0033.

If the direct reaction between ozone and TNB is assumed to be first order with respect to O_3 used, the reaction is written as

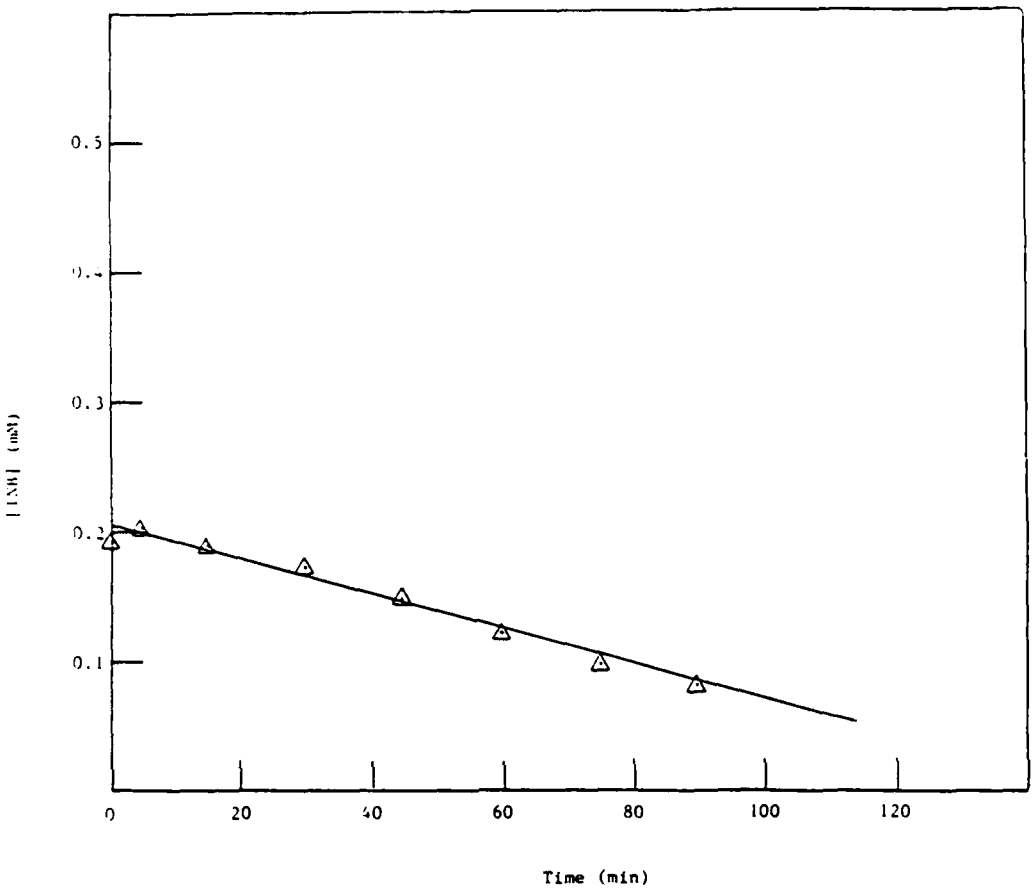

Figure 12. Concentration of TNB versus time with ozonation in the dark.

$[TNB]_0$ = 0.2 mM

O_3 Dose rate = 6.6×10^{-6} $M \cdot s^{-1}$

T_0 = 23°C

T_f = 23°C

pH_0 = 2.06

pH_f = 1.79

$$\text{TNB} + O_3 \xrightarrow{k_{O_3,\text{TNB}}} \alpha\ \text{TNB}_{ox} \qquad (41)$$

From this equation, the rate law and integrated form follow

$$-\alpha \frac{d(\text{TNB})}{dt} = k_{O_3,\text{TNB}}\, \alpha (\text{TNB})(O_3) \qquad (42)$$

$$\ln \frac{(\text{TNB})_o}{(\text{TNB})} = \alpha\, k_{O_3,\text{TNB}}\, (\bar{O}_3)\ t \qquad (43)$$

where α is the yield factor of TNB destruction per O_3 and $\bar{O}_3$ is the mean concentration during the reaction period t. The calculated rate constant for ozonation of TNB is 295 M^{-1} s^{-1} using the estimated yield factor and an average O_3 concentration in solution of 1.5×10^{-5} M. The rate constant for the consumption of O_3 is αk_{TNB} or $k_{O_3} = 9.7\ M^{-1}\ s^{-1}$. Aromatic compounds are also attacked by ozone but usually less readily than olefins [18]. Aromatic compounds behave as if the double bonds in the Kekule structures were actually there. However, substituents that withdraw electrons from the ring which include nitro, sulfonic, halogen and carbonyl groups deactivate the ring to ozone attack. Groups such as hydroxyl, alkyl and alkoxyl that are electron donors to the ring cause ring-activation toward ozone. Although rate constants for the consumption of ozone by molecules as complex as TNB are not available in the literature, the value calculated seems rather high when considering that the electron deficient nature of the TNB ring tends to make it unreactive with electrophilic reagents [19]. A possible reason for this

observation is that the overall oxidation process for direct ozonolysis may also involve oxygen, water and hydroxyl radicals that can accelerate the removal of TNB. The generation of dihydroxy peroxides and hydroperoxides are also possible through the Criegee mechanism involving unsaturated bonds [20]. The catalyzed O_3 decomposition process to oxidize TNB will be discussed more extensively in the following subsection.

Total organic carbon (TOC) analysis of the test solution at 120 minutes under the ozonation conditions described earlier and 0.2 mM initial TNB content gave a value of 6.0 mg/L TOC. The TNB standard (0.1 mM) had a TOC = 7.2 mg/L in agreement with the theoretical estimate. Thus, direct ozonation seemingly is effective in attacking the TNB ring structure. Analysis for solution nitrate after 120 minutes of ozonation gave a nitrate (NO_3^-) concentration of 6.3 mg/L which provides evidence that the ozone or reactive species generated by ozone can cleave the $C-NO_2$ bonds in this system.

4.3.3 TNB/O_3/UV System

The ozone photolysis experiments were done using the flow-through contacting and illumination arrangement. A number of different analytical techniques were employed to follow the course of the TNB oxidation. The first analytical results to be discussed are those of the GC/MS investigation. The experiment carried out in this study consisted of ozonation (at a dose rate of 6.6×10^{-6} $M \cdot s^{-1}$ at 500 $mL \cdot min^{-1}$) of a 0.2 mM TNB solution containing 0.01 M H_2SO_4 (pH 1.9). In this case, the rate of O_3 used was approximately 9.0×10^{-7} $M \cdot s^{-1}$ and the mean O_3 in solution was 2.1×10^{-6} M. The TNB concentration during the experiment is plotted vs. time in Figure 13. The initial TNB decay to below 20 percent is relatively linear with time. The kinetic parameter for TNB elimination will be discussed later in this subsection.

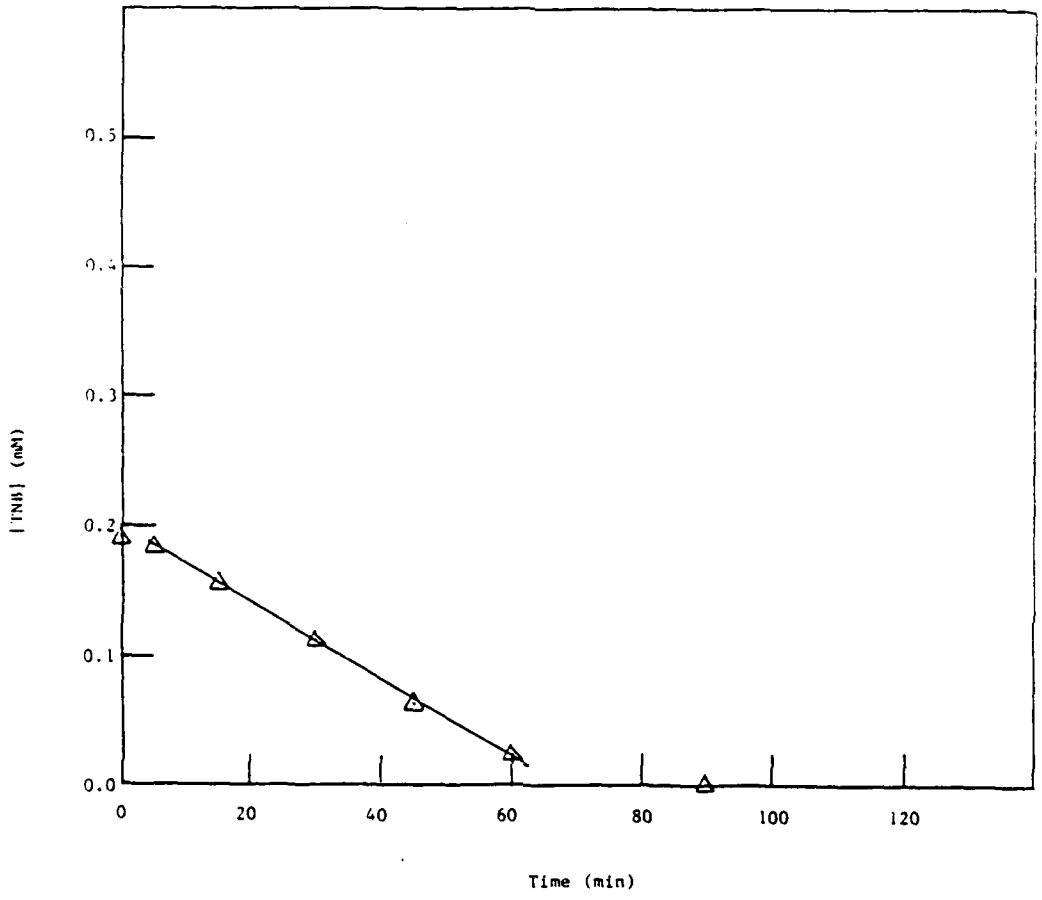

Figure 13. Concentration of TNB versus time with Ozone and UV irradiation.

$[TNB]_0$ = 0.2 mM

O_3 Dose rate = 6.6×10^{-6} $M \cdot s^{-1}$

I = 1.31 W/0.2L

T_0 = 23°C

T_f = 34°C

pH_0 = 1.85

pH_f = 1.80

Two samples of the above run (taken at 30 and 50 minutes) along with a zero time and distilled water (solvent) blank were analyzed by GC/MS using the two different chromatographic procedures described in Section 4.2.3. The results of this method showed that the TNB was present in all but the solvent blank but, no major TNB oxidation products were detected. The peroxides of ether found in all cases were obviously those introduced by the extraction solvent. Other contaminants included phthalate and silicon-containing compounds. There was however a trace of 1,3-dinitrobenzene found in the zero time sample which is probably an impurity in the source of the model compound TNB.

Analysis on the SP 1240 DA column showed that nitrophenol compounds were not present as reaction products. There are two types of carbon atoms in the TNB molecules; at the C-H and the $C-NO_2$ groups. The attack of hydroxyl radicals on the TNB molecule should generally occur at either the C-H or $C-NO_2$ bond. If the attack occurs on the C-H, a trinitrophenolic intermediate should be formed. But, if the $C-NO_2$ bond is cleaved then one would expect a dinitrobenzene intermediate or even a dinitrophenol product. Thus, since no nitrophenols were detected, these intermediate products must react very rapidly with additional radicals to produce smaller products.

Total organic carbon analysis of the 30 minute and 52 minute samples analyzed by GC/MS gave TOC values of 12 and 6 mg/L respectively. These data show that the TNB ring is destroyed at a much faster rate than observed for ozonation in the absence of UV illumination. Although the GC/MS analysis was unable to detect any TNB reaction products, the TOC results indicate that considerable total organic carbon remains in solution following the 52 minute O_3/UV treatment in spite of the near total elimination of TNB from solution. The confirmation of the presence of small acidic compounds as long term products in these oxidation systems will be presented in the next section.

Table 7 presents the results of nitrate analysis by ion chromatography. The concentration of nitrate at 30 minutes is consistent with the amount of TNB destroyed. However, at the later stages of the run, the nitrate appears to decrease from the earlier value and the amount found no longer corresponds to stoichiometric disappearance of TNB. This same behavior was noted for the TNB/H_2O_2/UV system and discussed in Section 4.2.

In addition to the O_3/UV system conditions used for the above experiments, other values of pH, O_3 dose rate, light intensity and temperature were investigated. In all of the experiments the initial concentration of TNB was 0.2 mM. Plots showing the TNB concentration during the course of the tests are presented in Appendix B. A list of the experimental conditions and some calculated system parameters for these tests is given in Table 8.

The ozone dose rate in mg O_3/L/min was calculated using the following equation

$$[O_3]_{dose} = \frac{(\text{gas volume/min})(\%\ O_3)(13.2\ \text{mg}\ O_3/\text{L}/\%)}{\text{reactor volume}} \qquad (44)$$

considering the ambient conditions of 23°C and 1.08 atm pressure. In Table 8 the dose rate has been converted to M/s for the 0.2 L volume reactor used. The total O_3 decomposition rate ($[O_3]_{used}$) is defined as the difference between $[O_3]_{dose}$ and the rate at which O_3 escapes the system in the exit gas. The average concentration of ozone in solution $[\bar{O}_3]_{sol}$ was determined using the Hoigne-Bader indigo method. The TNB concentration was followed by periodically complexing samples with sulfite and measuring the absorbance of the Meisenheimer complex.

TABLE 7. NITRATE ANALYSIS FOR O_3/UV/TNB EXPERIMENTS

Conditions	TNB Conc. (mM)	Time (min.)	NO_3^- (mg/L)
Control	0.2 plus 0.3 mM KNO_3	--	17
Baseline	0.2	0	< 0.5
O_3/UV	0.089	30	5.1
O_3/UV	0.00	52	4.7

TABLE 8. EXPERIMENTAL AND CALCULATED PARAMETERS FOR THE O_3/UV/TNB SYSTEM

Figure No.	pH[a]	$[O_3]_{dose}$ ($M \cdot s^{-1}$)	$[O_3]_{used}$ ($M \cdot s^{-1}$)	$[O_3]_{sol}$ (M)	$\frac{-d[TNB]_o}{}$ ($M \cdot s^{-1}$)	I_o[b,c] ($E \cdot s^{-1}$)	$[O_3]_{lm}$ ($M \cdot s^{-1}$)	D_{O_3}	h_{TNB}
M	2.06/1.79	6.6×10^{-6}	6.2×10^{-7}	1.5×10^{-5}	2.2×10^{-8}	--	--	--	0.035
R	1.85/1.80	6.6×10^{-6}	9.0×10^{-7}	2.1×10^{-6}	5.0×10^{-8}	1.2×10^{-7}	2.8×10^{-7}	2.3	0.055
B-1	5.67/3.11	6.6×10^{-6}	9.6×10^{-7}	9.1×10^{-6}	5.5×10^{-8}	5.1×10^{-7}	3.4×10^{-7}	0.67	0.057
B-2	9.67/3.15	6.6×10^{-6}	2.4×10^{-6}	1.1×10^{-5}	5.9×10^{-8}	6.1×10^{-7}	1.8×10^{-6}	2.9	0.024
B-3	1.86/1.73	1.3×10^{-5}	2.9×10^{-6}	3.5×10^{-6}	1.0×10^{-7}	2.0×10^{-7}	--	--	0.036
B-4	1.84/1.73	3.3×10^{-6}	1.2×10^{-6}	3.8×10^{-6}	3.1×10^{-8}	2.2×10^{-7}	--	--	0.026
B-5	1.78/1.73	6.6×10^{-6}	7.7×10^{-7}	6.6×10^{-6}	9.6×10^{-8}	1.4×10^{-7} *	1.5×10^{-7}	1.08	0.125
B-6	1.79/1.70	6.6×10^{-6}	6.3×10^{-7}	7.7×10^{-6}	5.2×10^{-8}	5.2×10^{-8} **	1.0×10^{-8}	0.20	0.082
B-7	1.79/1.74	6.6×10^{-6}	8.9×10^{-7}	3.3×10^{-6}	4.7×10^{-8}	1.9×10^{-7}	--	--	0.053

[a] pH initial and final

[b] $I_o = 1.39 \times 10^{-5}$ ein/S

[c] $e_{O_3} = 3314$, $e_{TNB} = 3000$

* $I_o = 55 \times 10^{-6}$ ein/S

** $I_o = 1.7 \times 10^{-6}$ ein/S

The incident light flux (λ = 254 nm) of the UV lamps were measured using the ferrioxalate actinometer method. The rate at which photons were absorbed by ozone (I_{O_3}) in solution containing the TNB substrate was calculated from the following equation, assuming Beer-Lambert's law is applicable at the O_3 and TNB concentrations used.

$$I_{O_3} = \frac{(O_3)\epsilon_{O_3} I_o}{(O_3)\epsilon_{O_3} + (TNB)\epsilon_{TNB}} \left(1 - 10^{-[(O_3)\epsilon_{O_3} + (TNB)\epsilon_{TNB}]}\right) \quad (45)$$

The quanta absorbed are in photons/mL/min, I_o is the incident light flux and ϵ is the molar extinction coefficient for the indicated solute. The amount of O_3 that is decomposed by photolysis ($[O_3]_{h\nu}$) is taken as the difference between $[O_3]_{used}$ in the UV experiment and the $[O_3]_{used}$ in the control ozonolysis without light (Figure 12). The assumption made here is that the direct ozonolysis rate for the given dose rate is not dependent on the pH or light intensity. Therefore this must be considered only an approximation.

The quantum yield for the decomposition of O_3 by UV light is expressed as follows.

$$\Phi_{O_3} = \frac{[O_3]_{h\nu}}{I_{O_3}} \quad (46)$$

The overall quantum yield for the destruction of TNB (η_{TNB}) by ozone, both direct ozonolysis and ozone photolysis, was calculated as the quotient of the TNB loss rate and $[O_3]_{used}$. The loss of TNB due to O_3 photolysis only $[(-d(TNB)^{h\nu}_{O_3})/dt]$ is estimated using the direct ozonolysis destruction rate. The quantum yield for TNB loss through the

decomposition of O_3 by light is given as $\eta^{h\nu}_{TNB}$. For the experiment in Figure 13, $\eta^{h\nu}_{TNB} = 0.1$.

Assuming the general model of Hoigne and Bader [19], the amount of hydroxyl radicals that is available for decomposition of TNB is determined by the amount of ·OH formed from O_3 photolysis and the relative rate with which ·OH reacts with TNB as compared to the rate at which ·OH is consumed by all other solutes. This is depicted below.

$$[O_3]_{h\nu} \longrightarrow \Phi_{O_3}\ (\cdot OH) \begin{cases} \longrightarrow k_{TNB}\ (TNB)(\cdot OH) \\ \longrightarrow \Sigma k_i (S_i)(\cdot OH) \end{cases} \qquad (47)$$

In this scheme, Φ_{O_3} is the yield for ·OH generation, i.e., the quantum yield for O_3 photolysis, k is the second order rate constant for reaction with ·OH and $\Sigma k_i(S_i)(\cdot OH)$ is the sum of the rate of ·OH scavenged by all solutes (S) including O_3 and TNB.

If the yield factor $\eta^{h\nu}_{TNB}$ which actually represents the fraction of ·OH radicals reacting with TNB is taken into account, then the rate of TNB removal by ·OH in the presence of competing scavengers is

$$\frac{-d(TNB)}{dt} = \Phi_{O_3} \eta_{TNB}^{h\nu} \left(\frac{d[O_3]_{h\nu}}{dt}\right) k_{TNB}\ (TNB)\ [\Sigma k_i(S_i)]^{-1} \qquad (4^{\circ})$$

If the conditions are such that $\Sigma k_i(S_i)$ is independent of the O_3 dose rate and concentration, and k_{TNB} (TNB) << $\Sigma k_i(S_i)$ then k_{TNB} can be directly determined from the above equation. The dominant competition reaction is considered to be the scavenging of $^{\cdot}OH$ by ozone. The value calculated for k_{TNB} for the experiment which had the same O_3 dose rate and temperature as the nonphotolytic ozonolysis run was 1.4×10^7 $M^{-1} \cdot s^{-1}$. This is to be taken as only an approximation considering the assumptions made. A more accurate evaluation of the TNB rate constant for reaction with $^{\cdot}OH$ is presented in the discussion of the hydrogen peroxide/UV.

The experimental results of tests conducted at different initial pH values showed that as the pH increased so too did the rate of O_3 consumption, the removal of TNB and the O_3 solubility. These observations are perhaps attributable to ozone removal catalyzed by hydroxide ions in direct agreement with the results of other aqueous ozone investigations [21]. The decrease in pH is consistent with the consumption of OH^-.

Other factors affecting the decomposition of TNB in solution were studied. Figure 14 shows that the TNB removal rate increases linearly with increasing ozone dose rate. However, this does not necessarily reflect an increase in the radical interactions but might be the effect of more ozonolysis. Different sizes of UV lamps were used to investigate the effect of light intensity influence on the O_3/UV destruction of TNB. The rate of TNB removal was found to be nearly

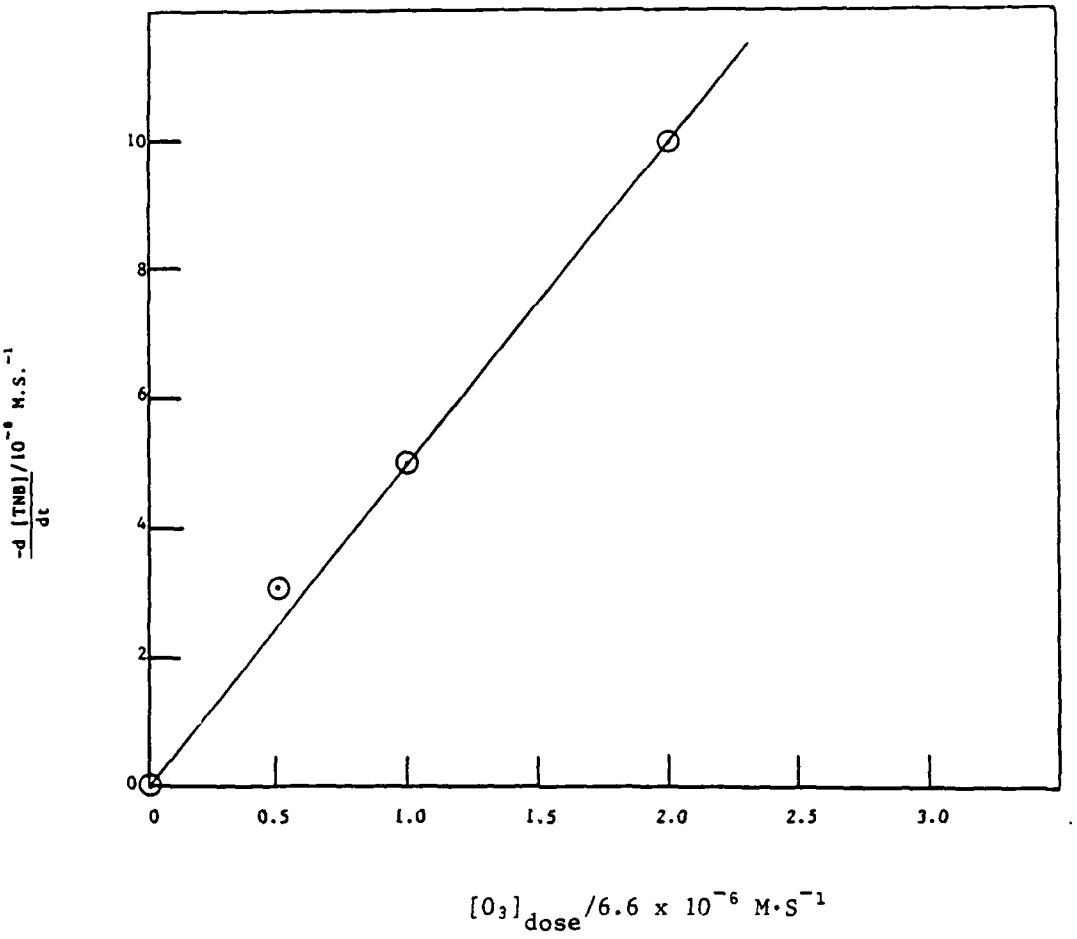

Figure 14. Decomposition of TNB versus Ozone dose rate $[O_3]_{dose}$

independent of intensity over the range 0.8 to 6.5 W/L. These results confirm that the increased substrate removal with higher dose rates is indeed due to a greater direct oxidation of TNB by ozone rather than enhanced reactions via radical intermediates. Raising the solution temperature to 70°C was also found to have no effect on the TNB removal process efficiency.

The average quantum yield for overall ozonation of TNB is Φ_{TNB} = 0.057 or in other words ~ 17.5 molecules of O_3 were consumed per molecule of TNB. Systems with the highest quantum yield for ozone photolysis did not give the highest yield for TNB removal, probably because of increased self-catalyzed consumption by O_3. Those cases where $\Phi_{O_3} > 2.0$, probably indicating chain reaction processes, should be noted.

4.4 Catalytic Ozone and Hydrogen Peroxide Systems

The generation of reactive oxy-radical species through non-photolytic catalysis offers hope of either replacing one of the high energy elements of existing oxidative treatment processes or of increasing the efficiency of an existing process, thus decreasing the energy or reagent requirements. Some of the potentially attractive systems investigated in this program include O_3/H_2O_2 with and without UV irradiation and particulate support catalysts. In addition, a few of the more common transition elements for H_2O_2 decomposition were investigated. The application of transition metal catalysis to fields such as wastewater cleanup is at a very early stage. The basic research literature that might be related to such applications is huge and rather chaotic. The effectiveness of these systems for the removal of 1,3,5-trinitrobenzene at an initial concentration of 0.2 mM was examined.

4.4.1 Ozone-Hydrogen Peroxide Decomposition (Direct and Photolytic)

The destruction of TNB through the decomposition reaction between O_3 and H_2O_2 was investigated. This reaction is known to produce hydroxyl radicals in the dark. The effect of both dark and UV irradiation conditions were examined. The experiments were carried out using a O_3 dose rate of 0.58 percent at 500 mL/min into the test solution containing 0.2 mM TNT, 0.01 M H_2SO_4 and 0.001 M H_2O_2. For the irradiated experiment the light intensity was 1.39×10^{-5} ein$\cdot s^{-1}$.

The resulting decay plots for the TNB and H_2O_2 concentrations under dark and irradiated conditions are shown in Figures 15 and 16 respectively. The removal rates for TNB were determined to be 3.8×10^{-8} M$\cdot s^{-1}$ in the dark and 6.8×10^{-8} M$\cdot s^{-1}$ under illumination.

The time required to reach a TNB level below 0.001 mM was 80 minutes for the dark run while for the irradiated run it took only 60

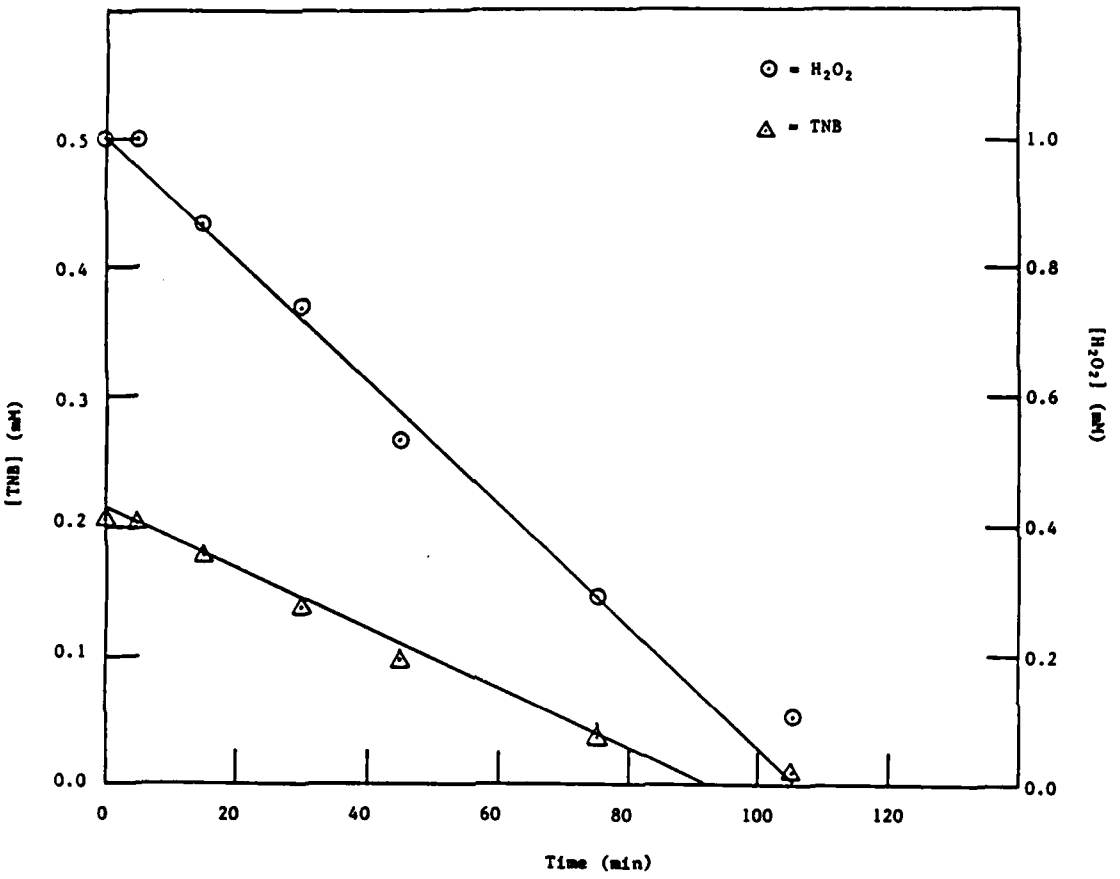

Figure 15. Concentration of TNB and H_2O_2 versus time with ozone in the dark.

$[TNB]_0$ = 0.2 mM

$[H_2O_2]_0$ = 1.0 mM

Ozone dose rate = 6.6×10^{-6} $M \cdot s^{-1}$

T_0 = 23°C

T_f = 23°C

pH_0 = 1.77

pH_f = 1.76

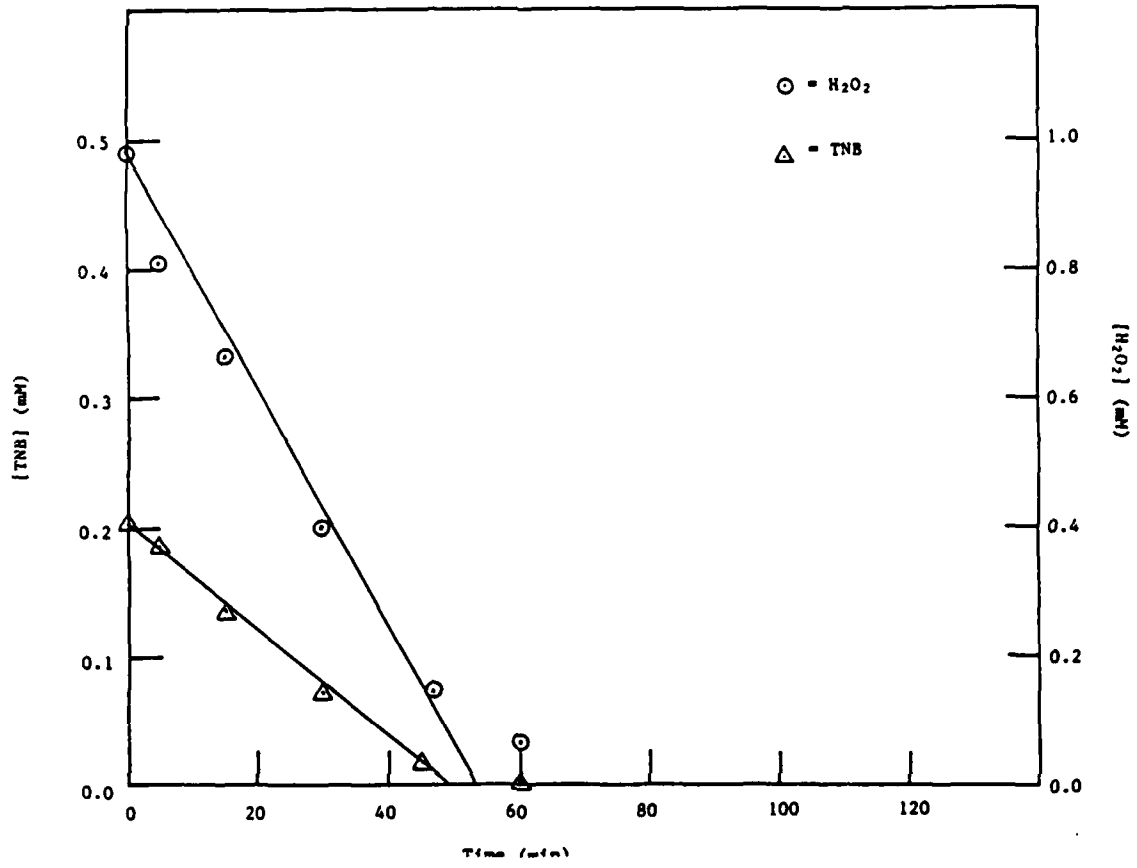

Figure 16. Concentration of TNB and H_2O_2 versus time with ozone and UV light.

$[TNB]_0$	= 0.2 mM
$[H_2O_2]_0$	= 1.0 mM
Ozone dose rate	= 6.6 x 10^{-6} x $M \cdot s^{-1}$
I	= 1.31 W/0.2L
T_0	= 23°C
T_f	= 36°C
pH_0	= 1.79
pH_f	= 1.76

minutes. Total organic carbon analysis of the above 80 and 60 minute samples gave 8 and 4.5 mg/L TOC respectively. These data suggest that the UV irradiation not only increases the removal rate of TNB but in addition also increases the oxidation rate of the TNB decomposition products. Nitrate analysis of 80 minute sample yielded a value of 6.3 mg/L which is consistent with the steady state value reached in the O_3/UV and H_2O_2/UV experiments and indicates cleavage of the aromatic ring structure.

The ozone-hydrogen peroxide system in the dark was also investigated using the same conditions as above except with an initial H_2O_2 concentration of 0.05 M. The experimental results during the course of the run are shown in Figure 17. The calculated removal rate for TNB (5.1×10^{-9} M·s^{-1}) is almost an order of magniture lower than when the H_2O_2 concentration was 0.001. This observation is attributed to the increased scavenging by the H_2O_2 of the hydroxyl radicals generated by the O_3/H_2O_2 decomposition. A similar effect of competition by H_2O_2 was found for the H_2O_2/UV system.

A list of the experimental results for the O_3/H_2O_2 tests are provided in Table 9, along with those of some previous experiments for comparison. Taking the direct ozonolysis of TNB as the baseline and comparing just the removal rates for TNB, the additional rate increase due to the present 0.001 M H_2O_2 is $\sim 1.6 \times 10^{-8}$ M·s^{-1} more than the baseline O_3 value of 2.2×10^{-8} M·s^{-1}. In the case of the ozonation with photolysis the TNB removal increased by 2.8×10^{-8} M·s^{-1}. When compared to the $O_3/UV/H_2O_2$ (0.001 M) system, ozone catalysis by photolysis alone was 1.8×10^{-8} M·s^{-1} slower in TNB removal, while ozone catalysis by H_2O_2 was lower by 3.0×10^{-8} M·s^{-1}. In other words, addition of 0.001 M H_2O_2 to the O_3/UV system increased the TNB destruction rate by 35 percent.

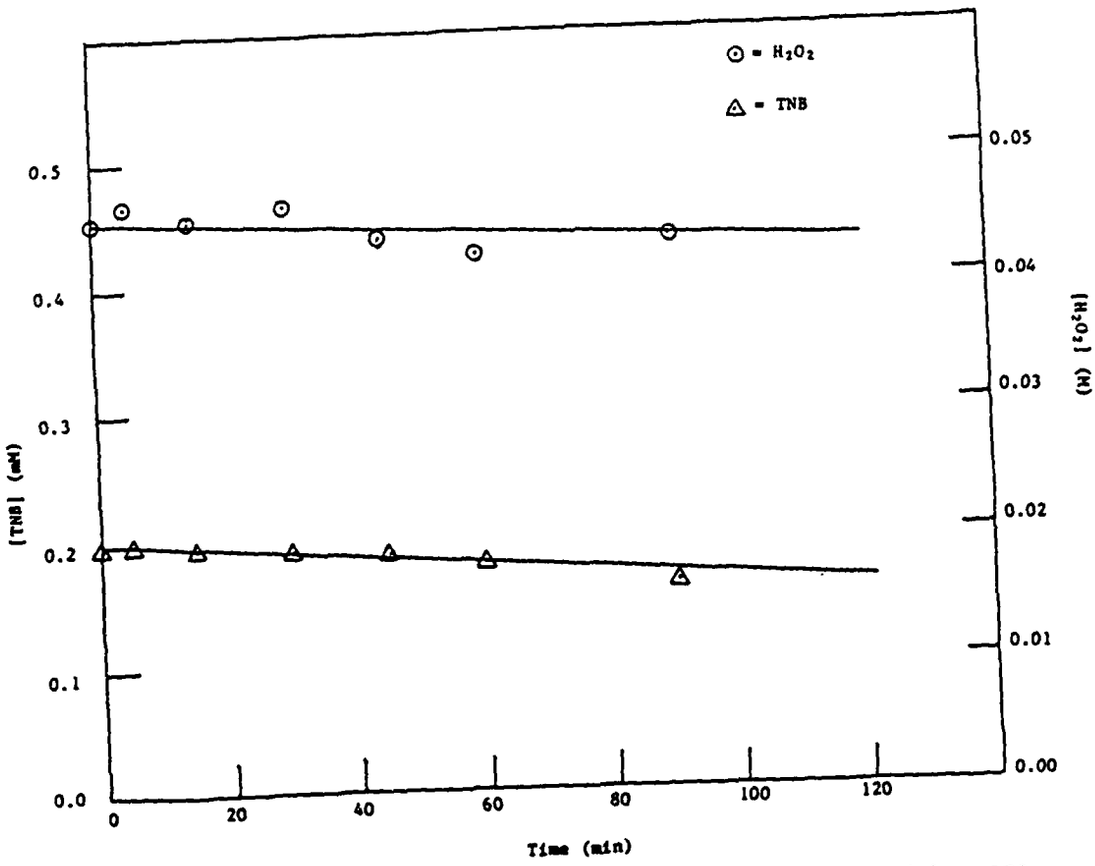

Figure 17. Concentration of TNB and H_2O_2 versus time with ozone in the dark.

$[TNB]_0$	= 0.2 mM
$[H_2O_2]_0$	= 0.05 M
Ozone dose rate	= 6.6×10^{-6} M·s^{-1}
T_0	= 23°C
T_f	= 23°C
pH_0	= 1.79
pH_f	= 1.88

TABLE 9. EXPERIMENTAL RESULTS FOR SOME O_3, H_2O_2 AND O_3/H_2O_2 SYSTEMS EXAMINED

System	$[H_2O_2]_o$ (M)	$[O_3]_{dose}$ ($M \cdot s^{-1}$)	$[O_3]_{used}$ ($M \cdot s^{-1}$)	$\overline{[O_3]}_{sol}$ (M)	$\frac{-d[H_2O_2]}{dt}$ ($M \cdot s^{-1}$)	$\frac{-d(TNB)}{dt}$ ($M \cdot s^{-1}$)	η_{TNB} #
O_3	--	6.6×10^{-6}	6.2×10^{-7}	1.5×10^{-5}	--	2.2×10^{-8}	0.035
O_3/UV	--	6.6×10^{-6}	9.0×10^{-7}	2.1×10^{-6}	2.2×10^{-8}	5.0×10^{-8}	0.055
H_2O_2/UV	0.05	--	--	--	4.0×10^{-6}	2.1×10^{-8}	0.005
O_3/H_2O_2	0.05	6.6×10^{-6}	7.9×10^{-7}	2.3×10^{-6}	2.8×10^{-7}	5.1×10^{-9}	0.018
O_3/H_2O_2	0.001	6.6×10^{-6}	8.8×10^{-7}	--	1.6×10^{-7}	3.8×10^{-8}	0.238
O_3/H_2O_2/UV	0.001	6.6×10^{-6}	1.1×10^{-6}	2.2×10^{-6} *	2.9×10^{-7}	6.8×10^{-8}	0.049

*Estimated value from baseline average.

#Overall yield per mole of reactant consumed.

Although the fastest TNB destruction rate occurred using the $O_3/UV/H_2O_2$ (0.001 M) system the highest quantum efficiency was found in the case of the dark O_3/H_2O_2 catalytic system. Only 4.2 moles of total reagent (O_3 + H_2O_2) were consumed per mole of TNB removed as compared to 20.4 moles per mole TNB for the $O_3/UV/H_2O_2$ (0.001 M) case. The lowest reagent efficiency was found for the H_2O_2 photolysis system (η_{TNB} = 0.005) where about 200 moles of H_2O_2 were consumed per mole TNB destroyed. This system, however, is probably subject to optimization.

4.4.2 Transition Metal Catalyzed H_2O_2 Decomposition

The influence of added transition metal cations was investigated using the H_2O_2 (0.05 M)/UV conditions for the removal of 1,3,5-trinitrobenzene from solution. The experiment involved adding 1 mM of Cu^{+2} ions as $CuSO_4$ to test solution. TOC analysis revealed that after 45 minutes into the run 9 mg/L TOc remained while the sample taken at 75 minutes showed only 6 mg/L remained cf., 14.4 mg/L TOC for 0.2 mM TNB. Thus, this system proved to be more effective than without the presence of Cu^{+2} ions.

The effect of adding Cu^{+2} ions to the H_2O_2/UV system (shown in Figure 18) was to increase the removal rate for both TNB and H_2O_2. The corresponding decay rates for TNB and H_2O_2 (5.1×10^{-8} $M \cdot s^{-1}$ and 3.0×10^{-5} $M \cdot s^{-1}$ respectively) were found to be the highest for H_2O_2/UV system. The quantum yield for H_2O_2 decomposition ($\eta_{H_2O_2}$ = 3.68) was also more than eight times greater than for the same system without Cu^{+2}. This rather substantial increase argues in favor of an oxidation process involving multi-chain reactions catalyzed by the transition metal cations.

Although this experiment resulted in the highest H_2O_2/UV destruction rate, the quantum efficiency was uneffected which means that the consumption process for $^{\cdot}OH$ by TNB proceeded in a similar manner as

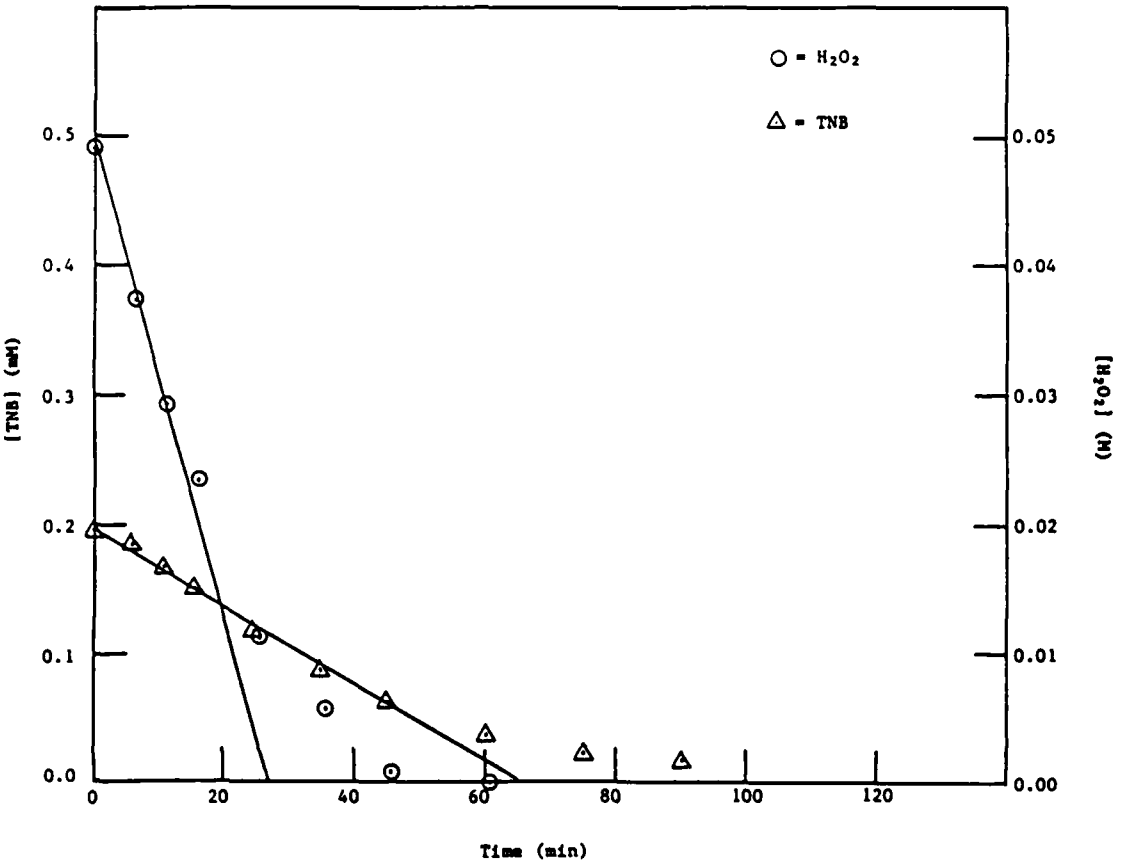

Figure 18. Concentration of TNB and H_2O_2 versus time with Cupric Sulfate (Cu SO_4) and Photolysis.

$[TNB]_0$ = 0.2 mM
$[H_2O_2]_0$ = 0.05 M
$[Cu\ SO_4]_0$ = 1.0 mM
I = 1.31 W/0.2L
T_0 = 23°C
T_f = 37°C
pH_0 = 1.80
pH_f = 1.69

in the uncatalyzed systems. A more indepth discussion of the H_2O_2-transition metal catalyzed system involving Fenton's reagent will be presented below.

While the added copper cations to solution was found to increase the H_2O_2 decomposition rate and subsequent TNB decay, the presence of the insoluble (particulate) catalyst Fe_2O_3 at the 1 gm/L level had virtually no influence on the decomposition rate of TNB and H_2O_2 as compared to the similar system without the Fe_2O_3. The reactant concentration vs. time are given in Figure 19. Using these results $-d(TNB)/dt = 1.8 \times 10^{-8}\ M \cdot s^{-1}$ and $-d(H_2O_2)/dt = 5.5 \times 10^{-6}$. The only speculation to be made from these data is that the iron atoms tied up in the oxide was unable to act as an H_2O_2 catalyst since free ferrous and ferric ions are known to be catalysts.

The combination of hydrogen peroxide and a ferrous salt, called "Fenton's reagent," has long been known to be an effective oxidant of a wide variety of organic substances. Although once in doubt, it now seems firmly established that hydroxyl radical is the actual oxidant in such systems [22, 23]. The system has in fact been used to determine the relative susceptibilities of various substrates to hydroxyl radical attack. The fact that hydrogen peroxide can be converted into the much more powerful oxidant without UV light stimulation makes Fenton's reagent an intriguing system. However, the ferrous ion is oxidized in the main process, and although it may be at least partially regenerated at a later stage, the overall reaction is not necessarily "catalytic" with regard to the iron redox state. Also, a number of side reactions are possible.

In the absence of oxygen, the following model is proposed for TNB oxidation by Fenton's reagent

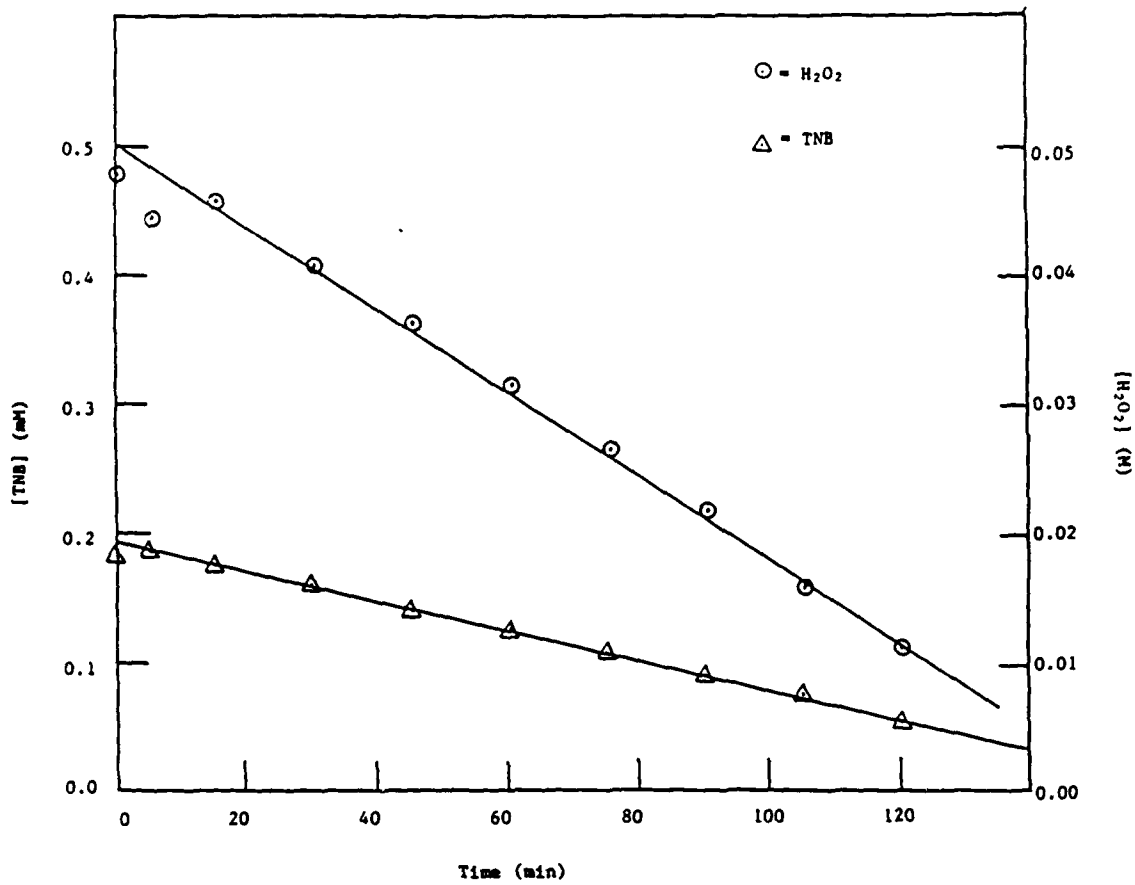

Figure 19. Concentration of TNB and H_2O_2 versus time with iron oxide (Fe_2O_3) and photolysis.

$[TNB]_0$ = 0.2 mM
$[H_2O_2]_0$ = 0.05 M
$[Fe_2O_3]$ = 6.25 mM
I = 1.31 W/0.2L
T_0 = 23°C
T_f = 33°C
pH_0 = 1.86
pH_f = 1.74

$$H_2O_2 + Fe^{+2} \xrightarrow{k_1} Fe^{+3} + \cdot OH + OH^- \qquad k_1 = 76 \qquad (49)$$

$$\cdot OH + H_2O_2 \xrightarrow{k_2} HO_2\cdot + H_2O \qquad k_2 = 3 \times 10^7 \qquad (50)$$

$$\cdot OH + Fe^{+2} \xrightarrow{k_3} Fe^{+3} + OH^- \qquad k_3 = 3 \times 10^8 \qquad (51)$$

$$\cdot OH + TNB \xrightarrow{k_{TNB}} (TNB)_{ox} \qquad k_{TNB} \qquad (52)$$

$$2(HO_2\cdot) \xrightarrow{k_4} H_2O_2 + O_2 \qquad k_5 = 8.6 \times 10^5 \qquad (53)$$

where the rate constants are given as $M^{-1}\cdot s^{-1}$. Oxygen tends to react with the intermediate radicals when present, upsetting the stoichiometry. Applying the steady-state hypothesis to d('OH)/dt and $d(HO_2')/dt$, yields expressions for the concentration of these radical species. The rate for H_2O_2 removal can ultimately be equated to

$$\frac{d(H_2O_2)}{dt} = - k_1 (H_2O_2)(Fe^{+2}) \qquad (54)$$

The rate constant relation for the overall TNB removal expression is given by

$$k_{TNB} = \frac{k_2(H_2O_2) + k_3(Fe^{+2})}{(TNB)\left[\frac{d(H_2O_2)}{d(TNB)} - 1\right]} \quad (55)$$

The Fenton's reagent experiments were investigated by adding H_2O_2 slowly to a nonquiesent solution containing excess ferrous ions and the TNB substrate. The test conditions were chosen to insure minimal influence by the competing reactions Eqs. 50 and 51. The experimental TNB and H_2O_2 concentration vs. time plots for an initial TNB concentration of 0.2 mM under acidic conditions are given in Figures 20 through 22. Spectroscopic analysis of the Fenton's reagent for ferric ions at the start of the experiments revealed that 50 percent of the initial ferrous concentration is oxidized to ferric ions after H_2O_2 addition is made. Other test conditions for the Fenton's reagent experiments and the calculated values for k_{TNB} are provided in Table 10. The average value for $k_{TNB} = 1.0 \times 10^8$ $M^{-1}.s^{-1}$ which is about an order of magnitude higher than the k_{TNB} estimated from the H_2O_2/UV experiments. The rate constant for k_{TNB} reaction with hydroxyl radicals might be affected by the somewhat secondary decomposition of H_2O_2 catalyzed by the ferric ions in solution. These catalyzed reactions can then generate hydroxyl radicals and other oxy-radical species that can increase the removal of TNB. At 180 minutes the 10 mM $FeSO_4$/5 mM H_2O_2 system had 8 mg/L TOC remaining. However, the best Fenton's reagent formulation was only half as effective in removing TNB as compared to the ozone photolyzed system.

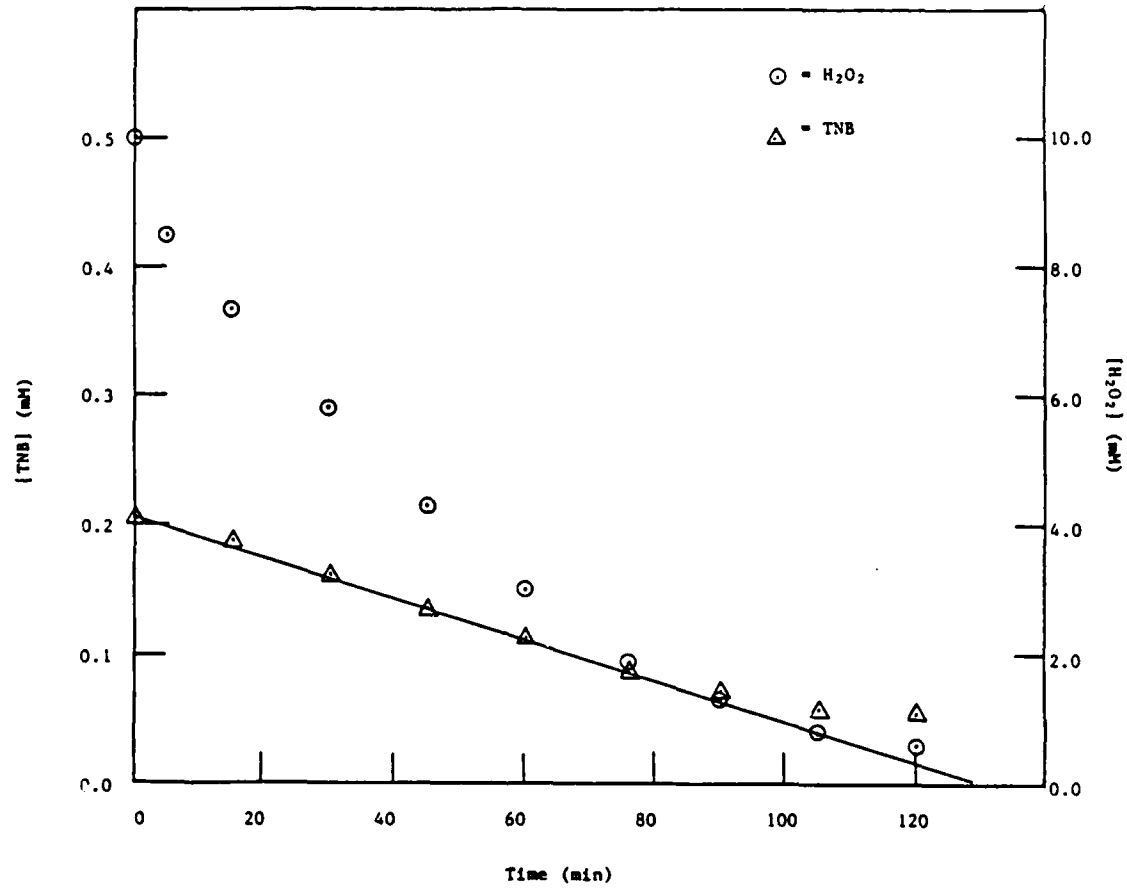

Figure 20. Concentration of TNB and H_2O_2 versus time with Fenton's Reagent ($FeSO_4$) in the dark.

$[TNB]_0$ = 0.2 mM
$[H_2O_2]_0$ = 10.0 mM
$[FeSO_4]$ = 20.0 mM
T_0 = 23°C
T_f = 23°C
pH_0 = 1.80
pH_f = 1.78

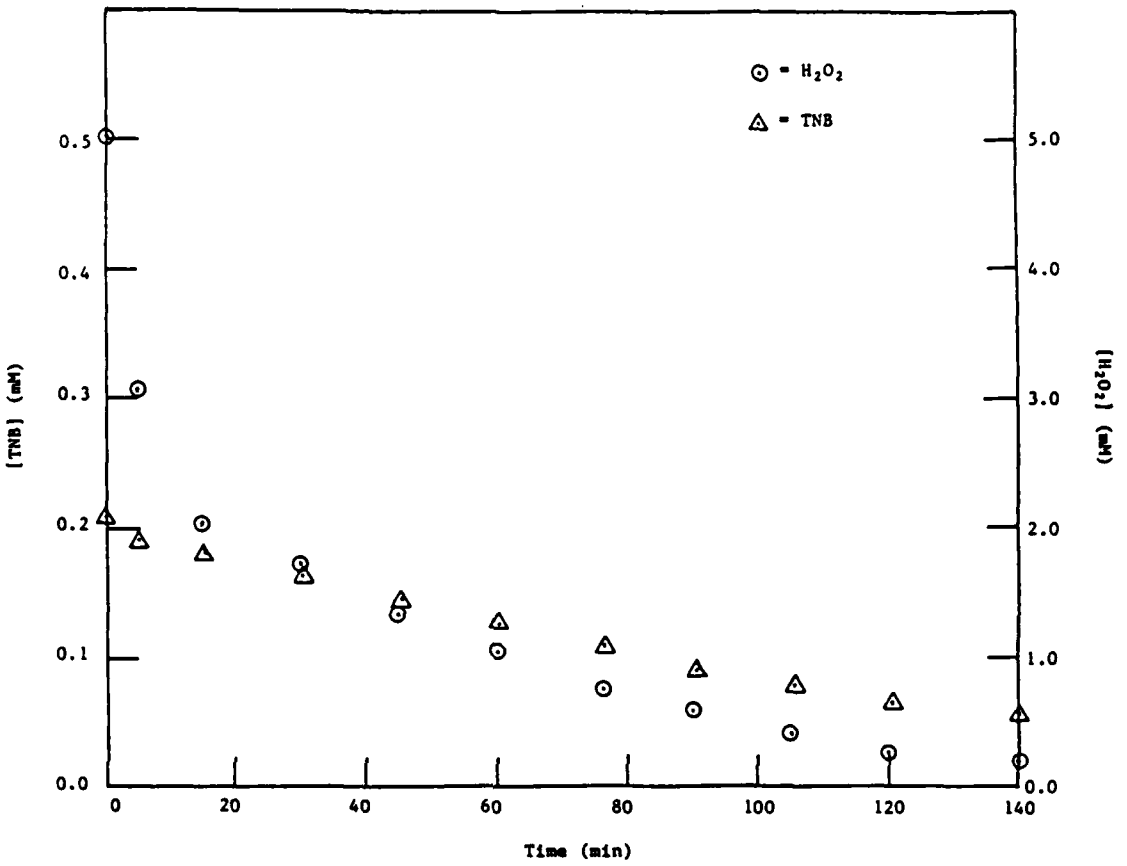

Figure 21. Concentration of TNB and H_2O_2 versus time with Fenton's Reagent ($FeSO_4$) in the dark.

$[TNB]_0$ = 0.2 mM

$[H_2O_2]_0$ = 5.0 mM

$[FeSO_4]$ = 10.0 mM

T_0 = 23°C

T_f = 23°C

pH_0 = 1.85

pH_f = 1.81

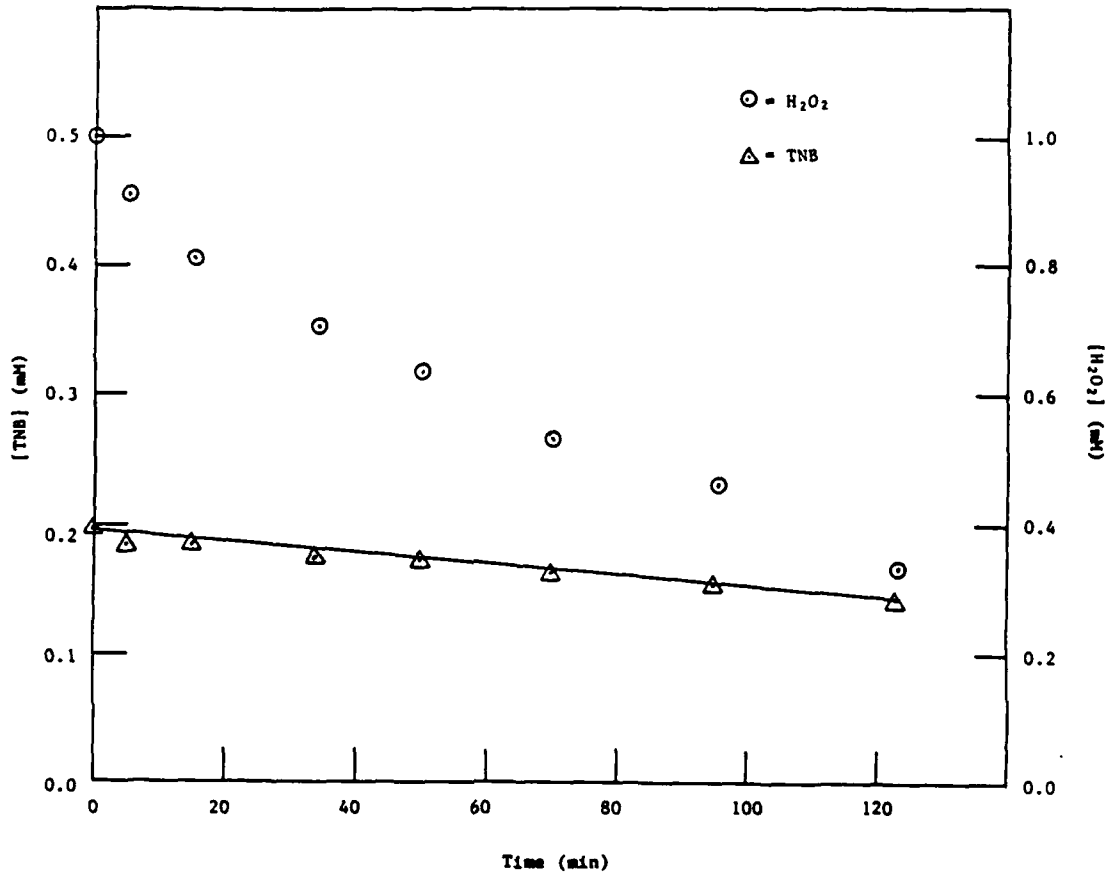

Figure 22. Concentration of TNB and H_2O_2 versus time with Fenton's Reagent in the dark.

$[TNB]_0$ = 0.2 mM
$[H_2O_2]_0$ = 1.0 mM
$[FeSO_4]$ = 2.0 mM
T_0 = 23°C
T_f = 23°C
pH_0 = 1.84
pH_f = 1.81

TABLE 10. EXPERIMENTAL AND KINETIC PARAMETERS FOR FENTON'S REAGENT EXPERIMENTS WITH 0.2 mM TNB at pH 1.8

$(FeSO_4)$ (mM)	(H_2O_2) (mM)	$\frac{-d(H_2O_2)}{dt}$ ($M \cdot s^{-1}$)	$\frac{-d(TNB)}{dt}$ ($M \cdot s^{-1}$)	k_{TNB} ($M^{-1} \cdot s^{-1}$)
20	10	3.1×10^{-6}	2.5×10^{-8}	1.5×10^{8}
10	5	3.2×10^{-6}	2.0×10^{-8}	5.0×10^{7}
2	1	1.1×10^{-7}	6.8×10^{-9}	1.0×10^{8}

REFERENCES

1. C. G. Hatchard and C. A. Parker, Proc. Roy Soc. (London) A, 235, 518 (1956).

2. R. Gl Parker, J. M. McOwen and J. A. Cherolis, J. Forensic Sci., 20(2), 254 (1975).

3. J. Pearson, E. Harold and P. R. Singer, JAWWA, 66, 600 (1974).

4. H. Bader and J. Hoigne, Water Res., 15, 449 (1981).

5. P. O. Bethge and K. Lindstrom, Analyst, 99, 137 (1974).

6. M. A. Ronning, R. L. Atkins and C. A. Heller, J. Photochem. 9, 403 (1978).

7. O. Sandus and N. Slagg, "Reactions of Aromatic Nitro Compounds. 1. Photochemistry," Tech Rep No. 4385 (1962).

8. J. H. Baxendale and J. S. Wilson, Tran. Faraday Soc., 53, 344 (1957).

9. D. H. Volman and J. C. Chen, J. Am. Chem. Soc., 81, 4141 (1959).

10. M. Hatada, I. Kraljic, A. El-Samahy and C. N. Trumbore, J. Phys. Chem., 78, 888 (1974).

11. J. P. Hunt and H. Taube, J. Am. Chem. Soc., 74, 5999 (1952).

12. F. Haber and J. Weiss, Proc. Royal Soc. (London) A, 147, 332 (1934).

13. J. Hoigne and H. Bader, Envir. Sci. Tech., 12, 79 (1978).

14. D. T. Sawyer and J. S. Valentine, Acc. Chem. Res., 14, 393 (1981).

15. F. S. Dainton and J. Rowbottom, Trans. Faraday Soc., 49, 1160 (1953).

16. C. C. Andrews and J. L. Osman, "The Effects of UV Light on TNT and Other Explosives in Aqueous Solution," Tech. Rep. No. WQEC/C77-32 (1977).

17. J. Hoigne and H. Bader, Water Res., 10, 377 (1976).

18. P. S. Bailey, Chem. Rev., 58, 957 (1958).

19. J. Hoigne and H. Bader, Water Res., 17, 178 (1983) and 17, 185 (1983).

20. R. Criegee, Angew. Chem. Int. Ed. Engl., 14, 745 (1975).

21. L. Forni, D. Bahnemann and E. J. Hart, J. Phys. Chem., 86, 255 (1982).

22. C. Walling, Acc. Chem. Res., 8, 125 (1975).

23. M. E. Snook and G. A. Hamilton, J. Am. Chem. Soc., 96, 860 (1974).

APPENDIX A

TNB CONCENTRATION VS. TIME PLOT FOR TNB/H_2O_2/UV SYSTEMS

Figures A-1 through A-7

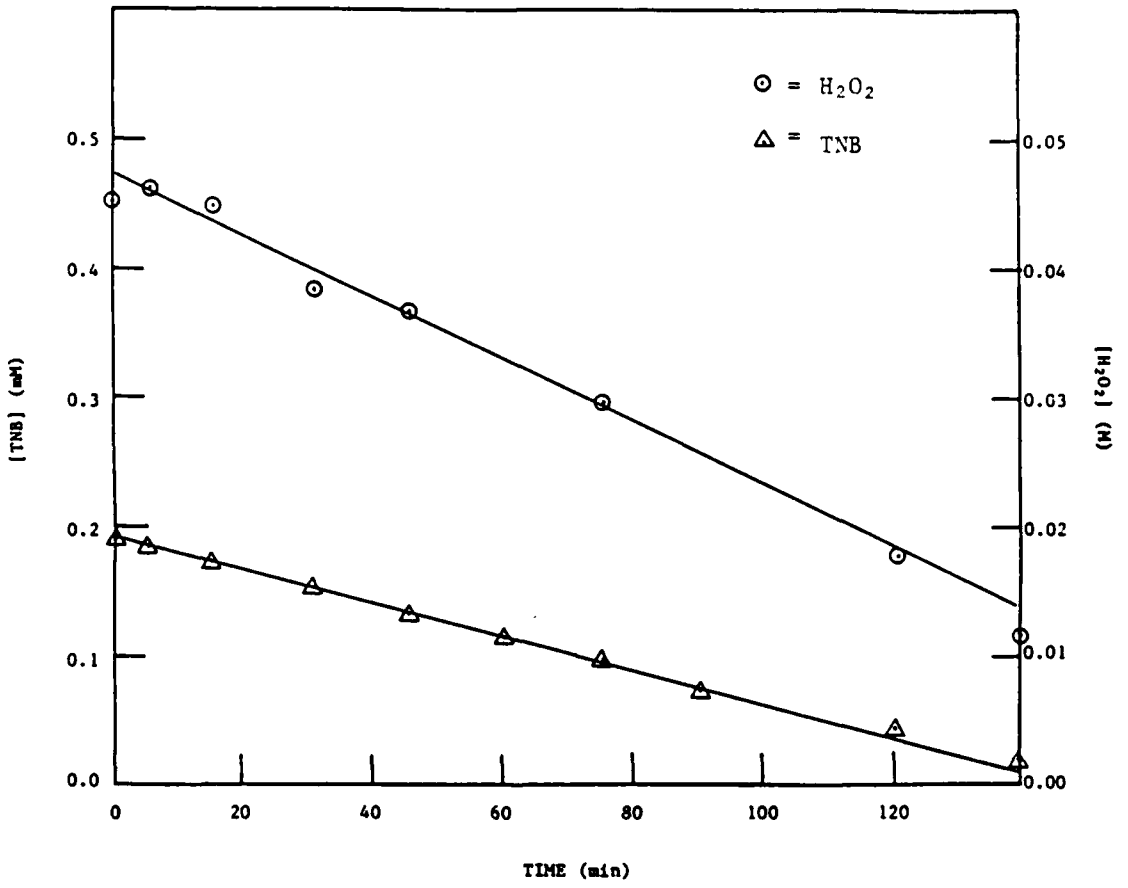

Figure A-1. Concentration of TNB and H_2O_2 versus time with UV light.

$[TNB]_0$ = 0.2 mM

$[H_2O_2]_0$ = 0.05 M

I = 1.31 W/0.2L

T_0 = 23°C

T_f = 34°C

pH_0 = 1.84

pH_f = 1.74

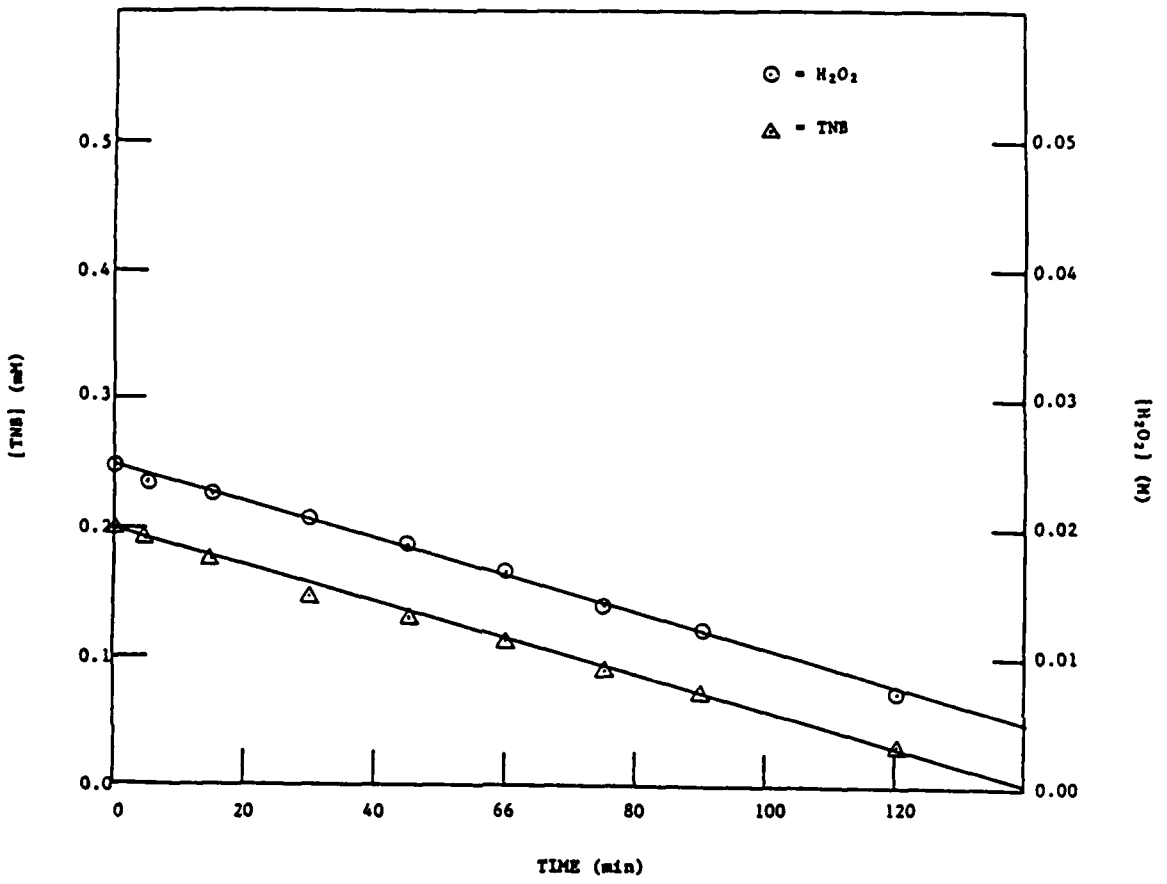

Figure A-2. Concentration of TNB and H_2O_2 versus time with UV light.

[TNB] = 0.2 mM

$[H_2O_2]$ = 0.025 M

I = 1.31 W/0.2L

T_0 = 23°C

T_f = 34°C

pH_0 = 1.86

pH_f = 1.77

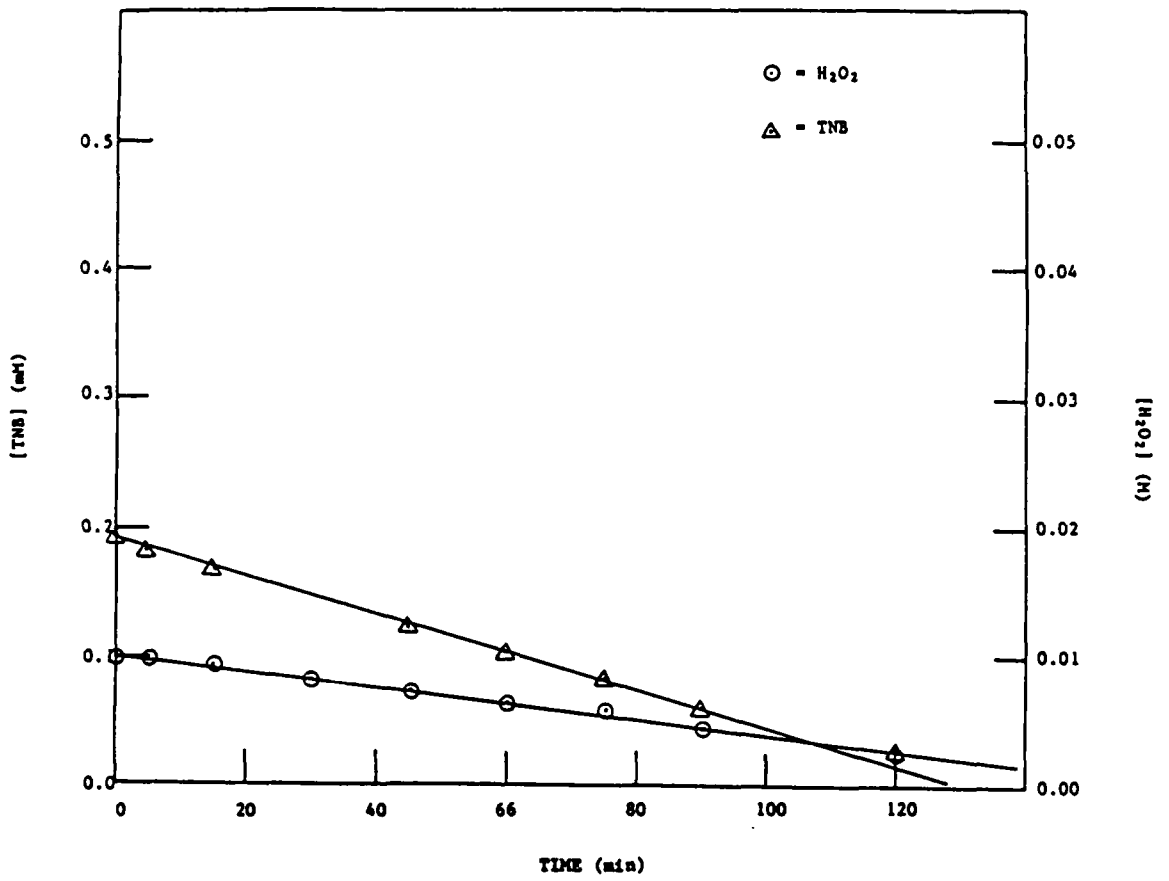

Figure A-3. Concentration of TNB and H_2O_2 versus time with UV light.

[TNB] = 0.2 mM

$[H_2O_2]$ = 0.01 M

I = 1.31 W/0.2L

T_0 = 23°C

T_f = 34°C

pH_0 = 1.82

pH_f = 1.74

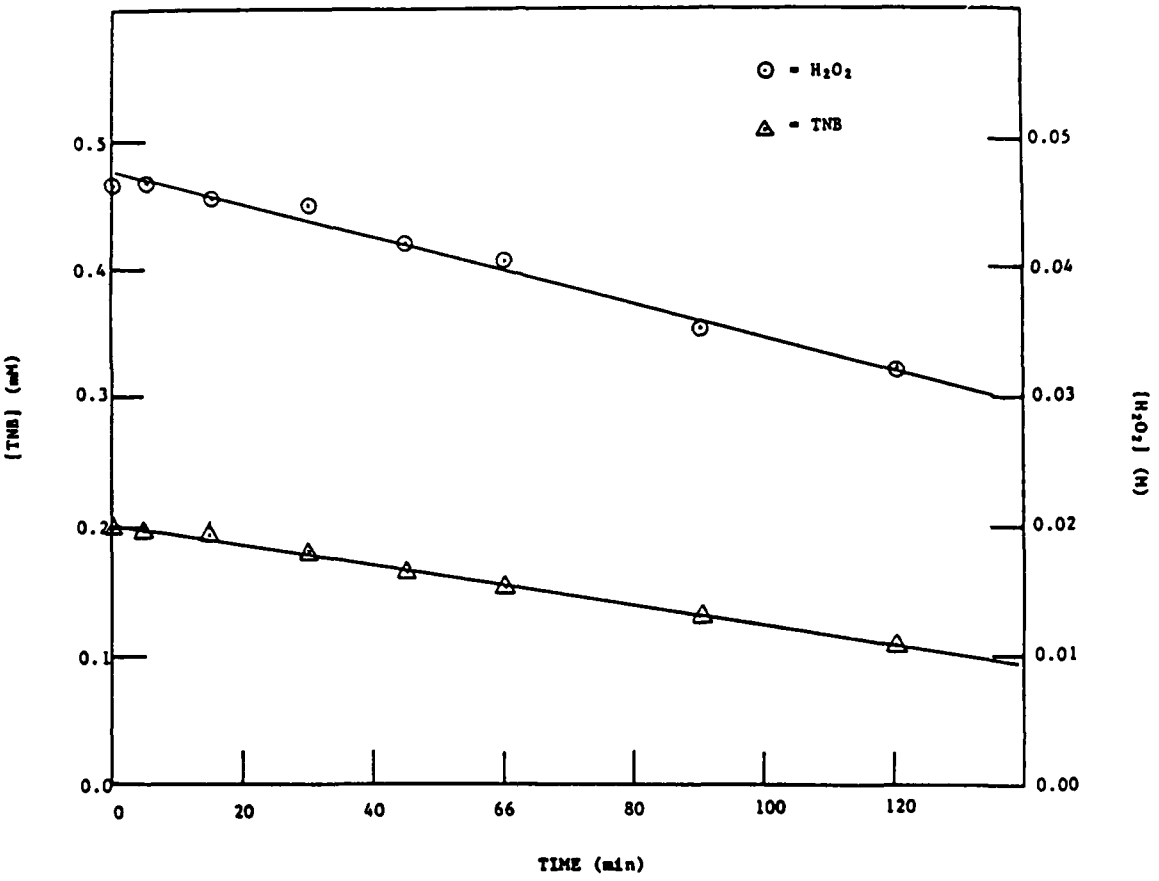

Figure A-4. Concentration of TNB and H_2O_2 versus time with UV light.

$[TNB]_0$ = 0.2 mM

$[H_2O_2]_0$ = 0.05 M

I = 0.52 W/0.2L

T_0 = 23°C

T_f = 32°C

pH_0 = 1.87

pH_f = 2.00

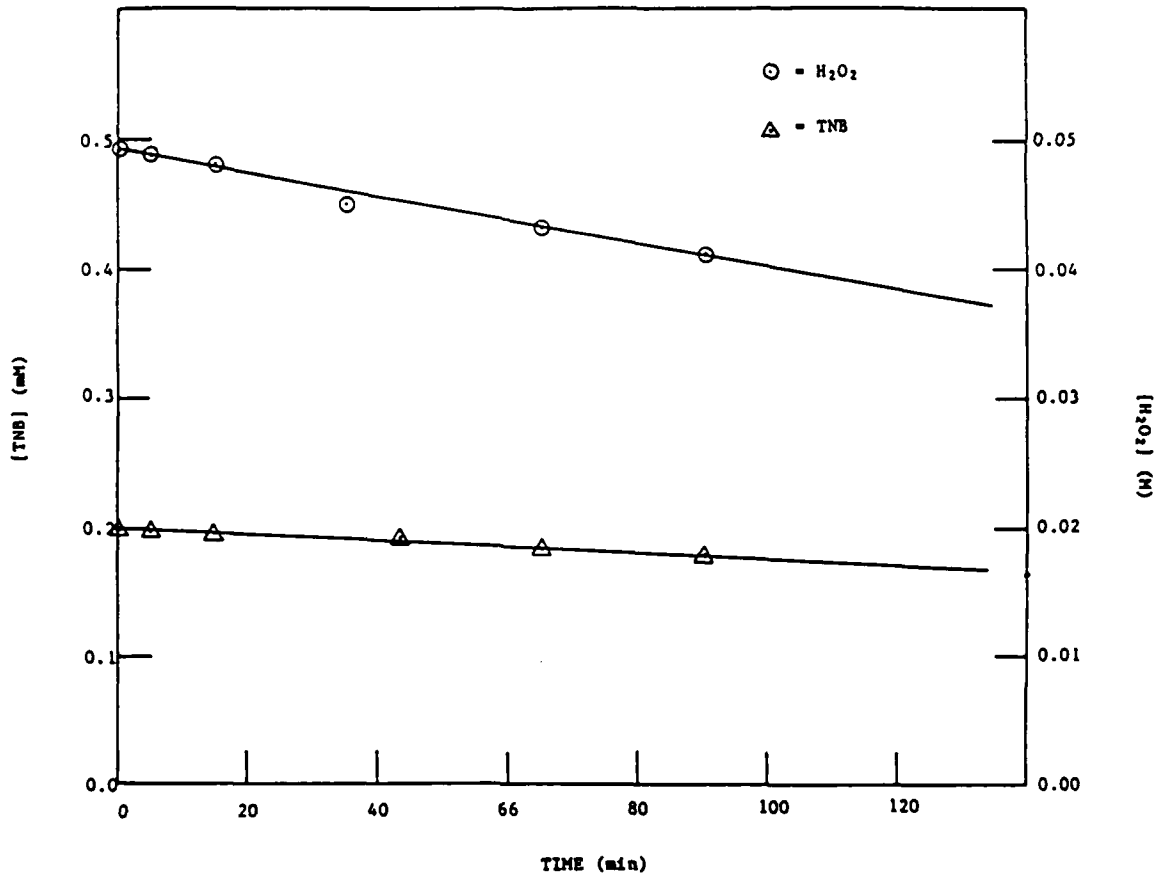

Figure A-5. Concentration of TNB and H_2O_2 versus time with UV light.

$[TNB]_0$ = 0.2 mM

$[H_2O_2]_0$ = 0.05 M

I = 0.16 W/0.2L

T_0 = 23°C

T_f = 33°C

pH_0 = 1.85

pH_f = 1.75

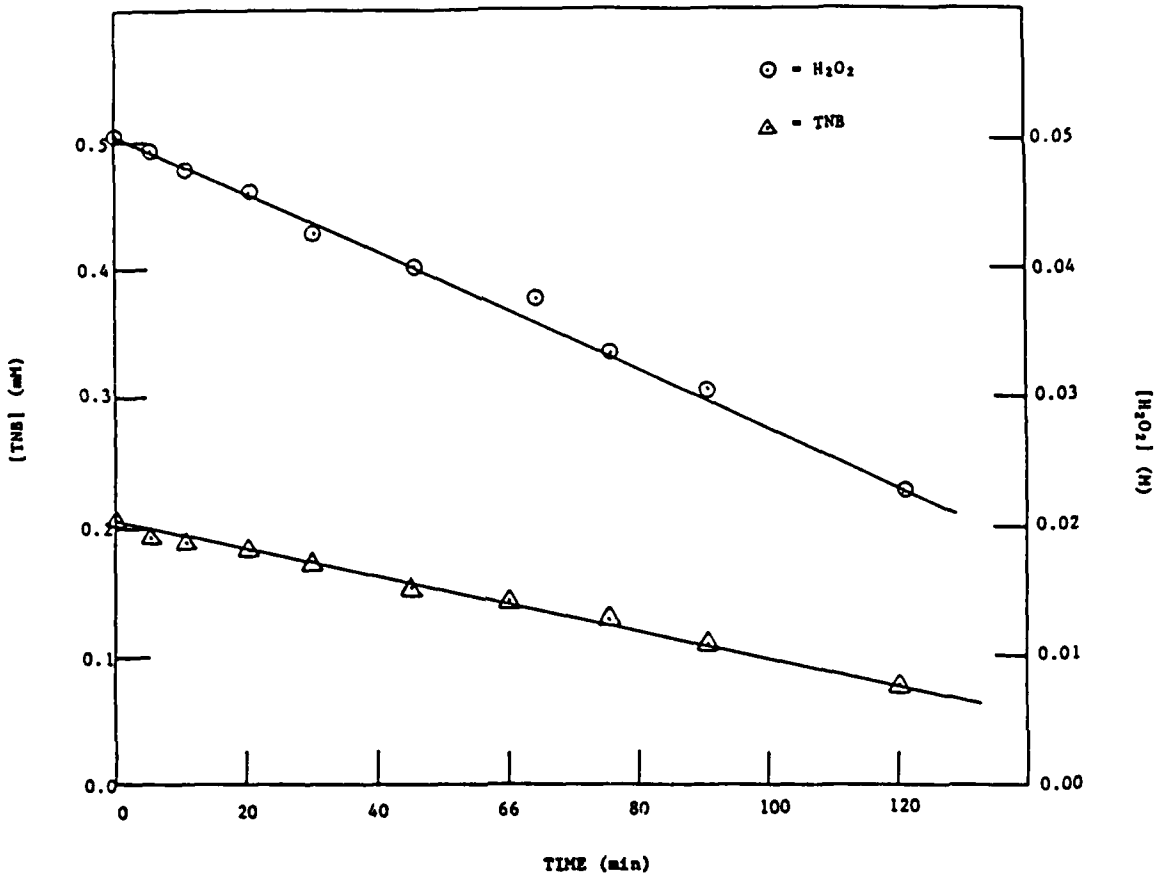

Figure A-6. Concentration of TNB and H_2O_2 versus time with UV light and neutral pH.

[TNB] = 0.2 mM

$[H_2O_2]$ = 0.05 M

I = 1.31 W/0.2L

T_0 = 23°C

T_f = 34°C

pH_0 = 5.65

pH_f = 3.26

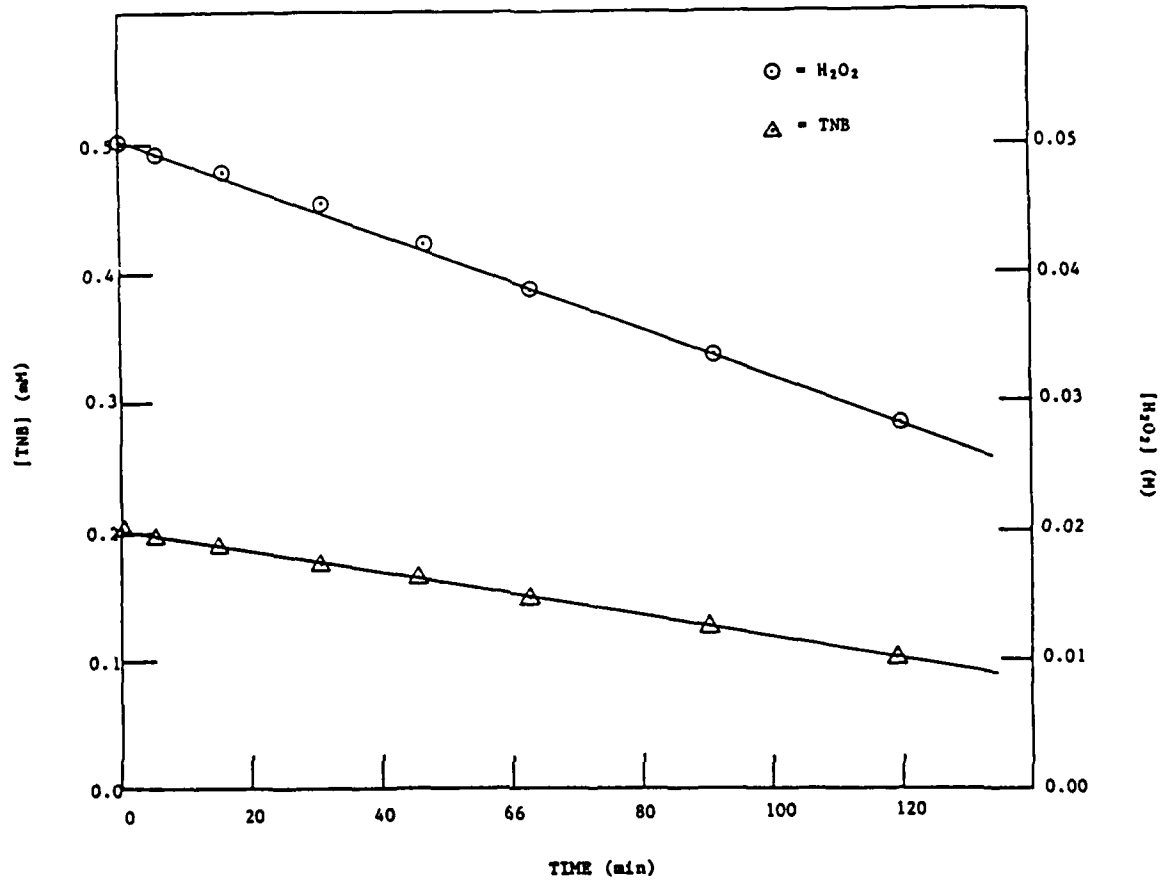

Figure A-7. Concentration of TNB and H_2O_2 versus time with UV light and at elevated temperature.

$[TNB]_0$ = 0.2 mM

$[H_2O_2]_0$ = 0.05 M

I = 1.31 W/0.2L

Temp. = 70°C

pH_0 = 1.85

pH_f = 1.72

AD-A141 703 LITERATURE SURVEY: BASIC MECHANISMS OF EXPLOSIVE COMPOUNDS IN WASTEWATER(U) SUMX CORP AUSTIN TX D W DEBERRY ET AL. MAY 84 SUMX-C82-121

2/2

UNCLASSIFIED DRXTH-TE-CR-84279 DAAK11-83-C-0006 F/G 13/2 NL

END
DATE FILMED
7-84
DTIC

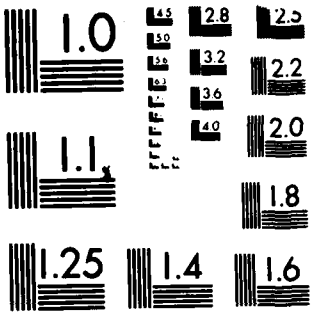

APPENDIX B

CONCENTRATION VS. TIME PLOTS FOR TNB/O_3/UV SYSTEMS

Figures B-1 through B-7

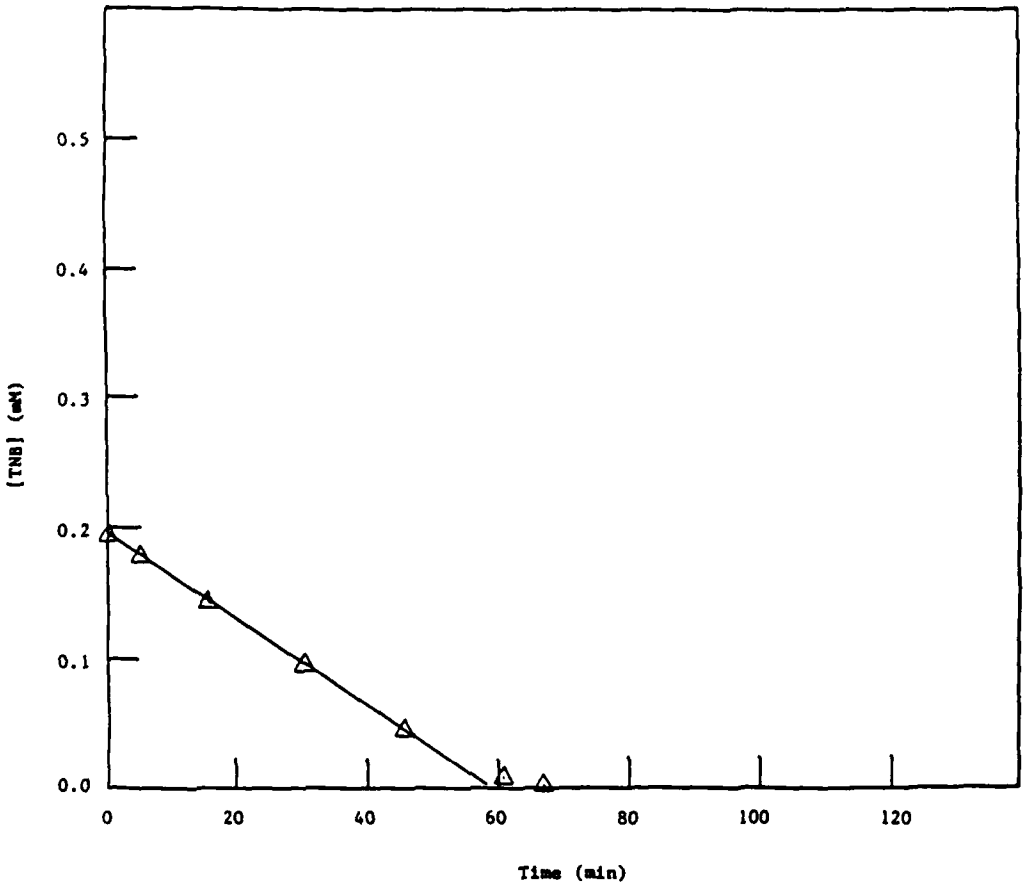

Figure B-1. Concentration of TNB versus time with ozone, photolysis, and neutral pH.

$[TNB]_0$ = 0.2 mM

Ozone dose rate = 6.6×10^{-6} $M \cdot s^{-1}$

I = 1.31 W/0.2L

T_0 = 23°C

T_f = 33°C

pH_0 = 5.67

pH_f = 3.11

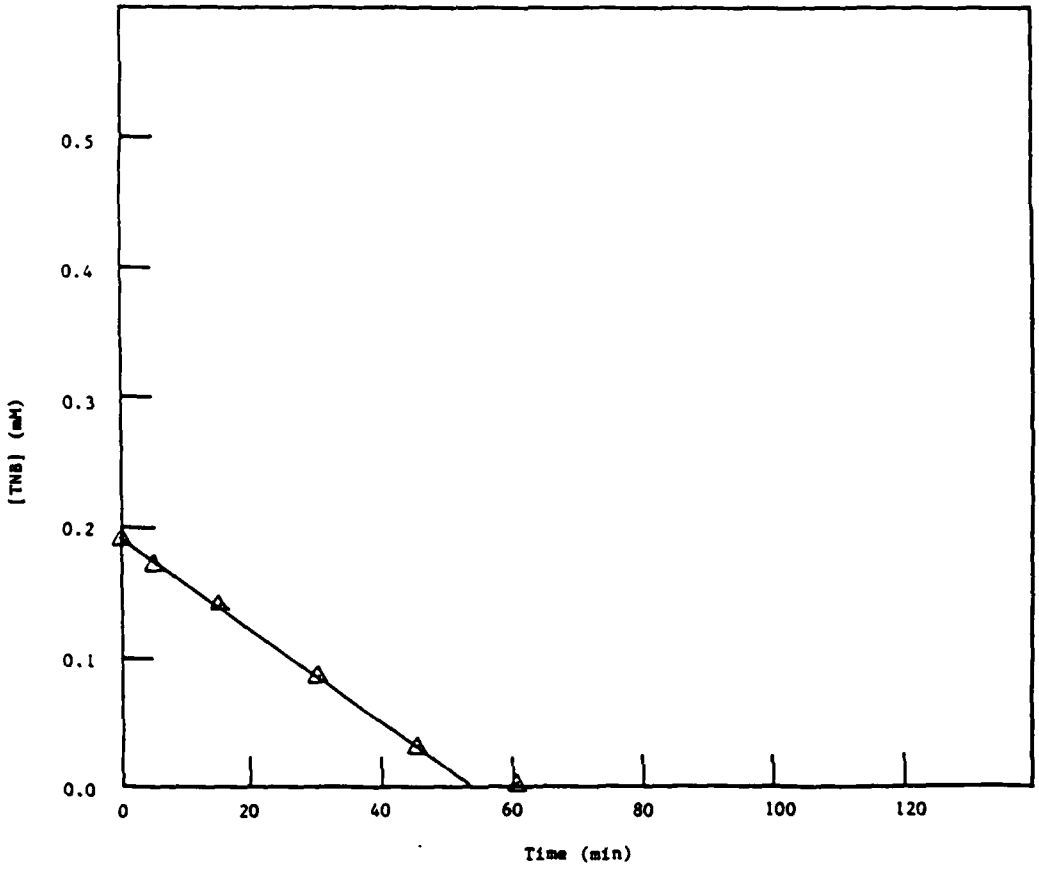

Figure B-2. Concentration of TNB versus time with ozone, photolysis, and at a high pH (9.67).

$[TNB]_0$	= 0.2 mM
Ozone dose rate	= 6.6×10^{-6} $M \cdot s^{-1}$
I	= 1.31 W/0.2L
T_0	= 23°C
T_f	= 34°C
pH_0	= 9.67
pH_f	= 3.15

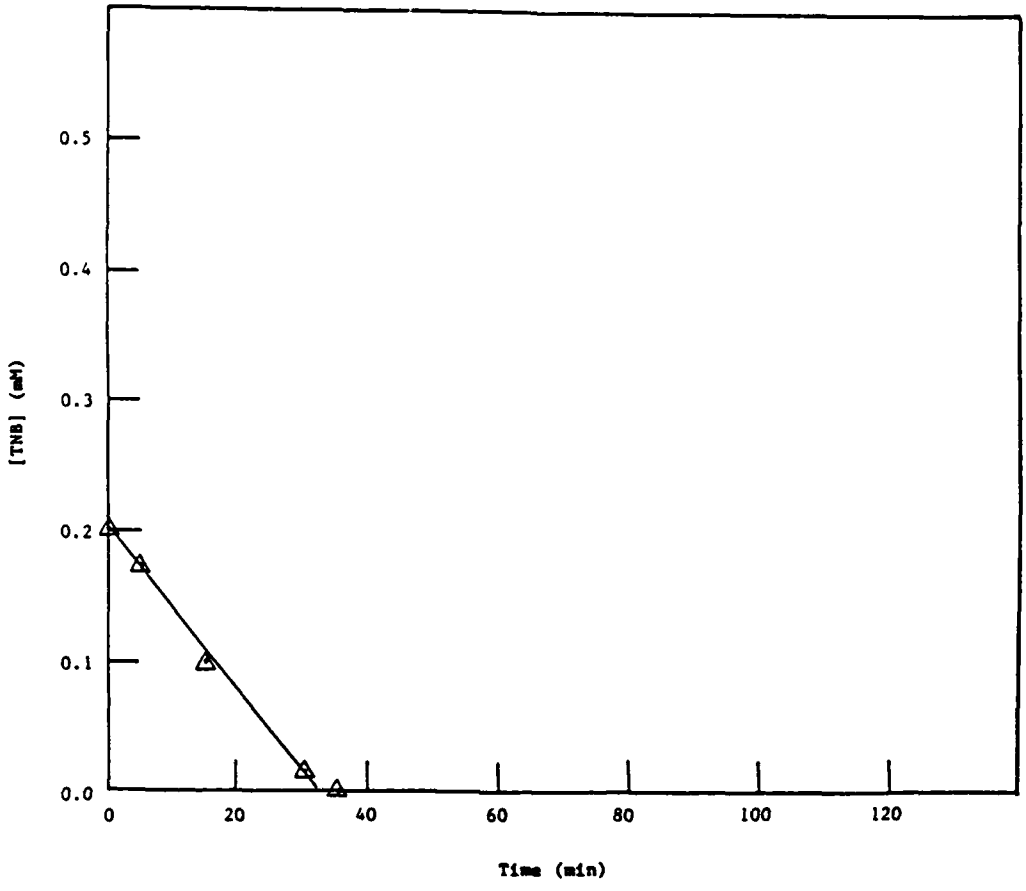

Figure B-3. Concentration of TNB versus time with ozone and photolysis.

$[TNB]_0$ = 0.2 mM

Ozone dose rate = 1.3×10^{-5} $M \cdot s^{-1}$

I = 1.31 W/0.2L

T_0 = 23°C

T_f = 34°C

pH_0 = 1.86

pH_f = 1.73

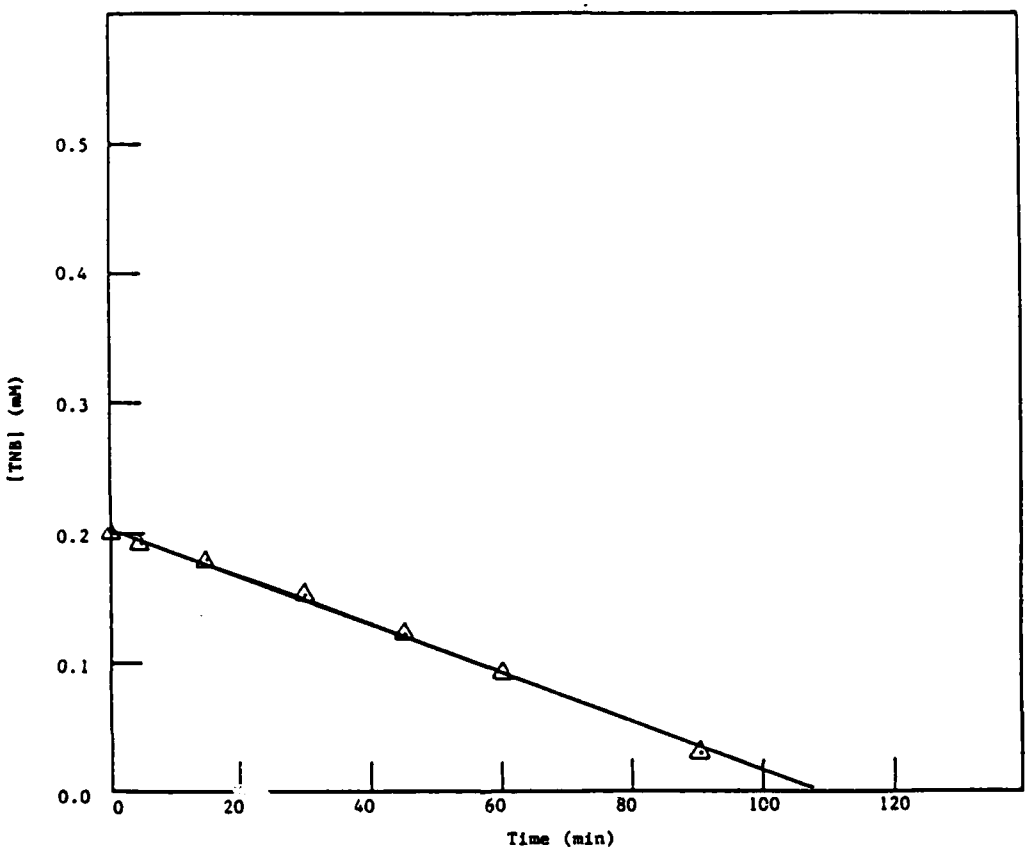

Figure B-4. Concentration of TNB versus time with ozone and photolysis.

$[TNB]_0$ = 0.2 mM

Ozone dose rate = 3.3×10^{-6} M·s^{-1}

I = 1.31 W/0.2L

T_0 = 23°C

T_f = 34°C

pH_0 = 1.84

pH_f = 1.73

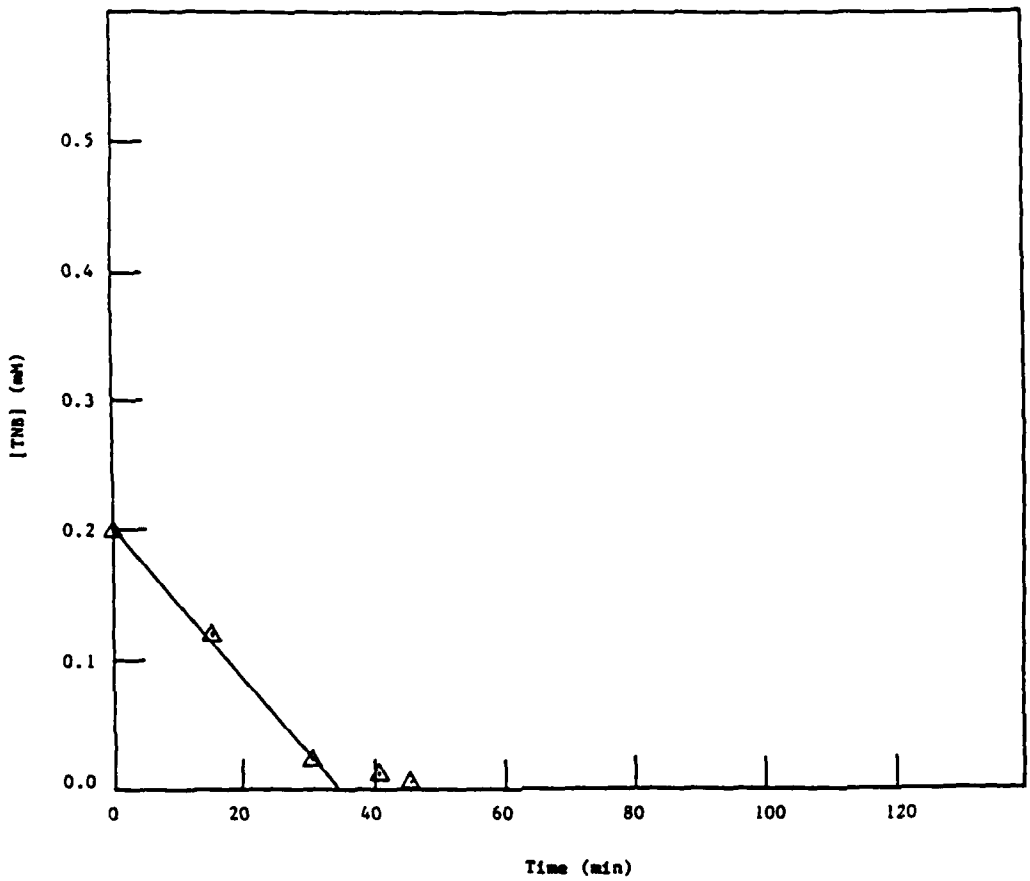

Figure B-5. Concentration of TNB versus time with ozone and photolysis.

$[TNB]_0$	= 0.2 mM
Ozone dose rate	= 6.6×10^{-6} M·s^{-1}
I	= 0.52 W/0.2L
T_0	= 23°C
T_f	= 32°C
pH_0	= 1.78
pH_f	= 1.73

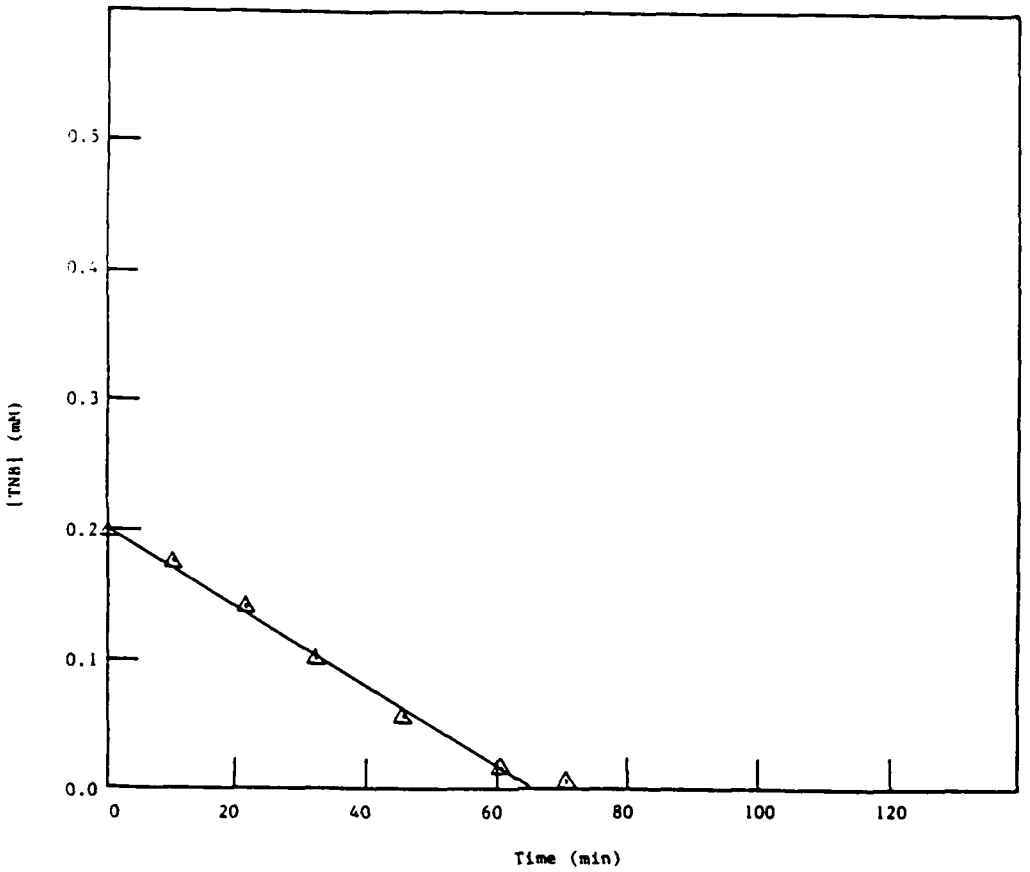

Figure B-6. Concentration of TNB versus time with ozone and photolysis.

$[TNB]_0$ = 0.2 mM

Ozone dose rate = 6.6×10^{-6} $M \cdot s^{-1}$

I = 0.16 W/0.2L

T_0 = 23°C

T_f = 32°C

pH_0 = 1.79

pH_f = 1.70

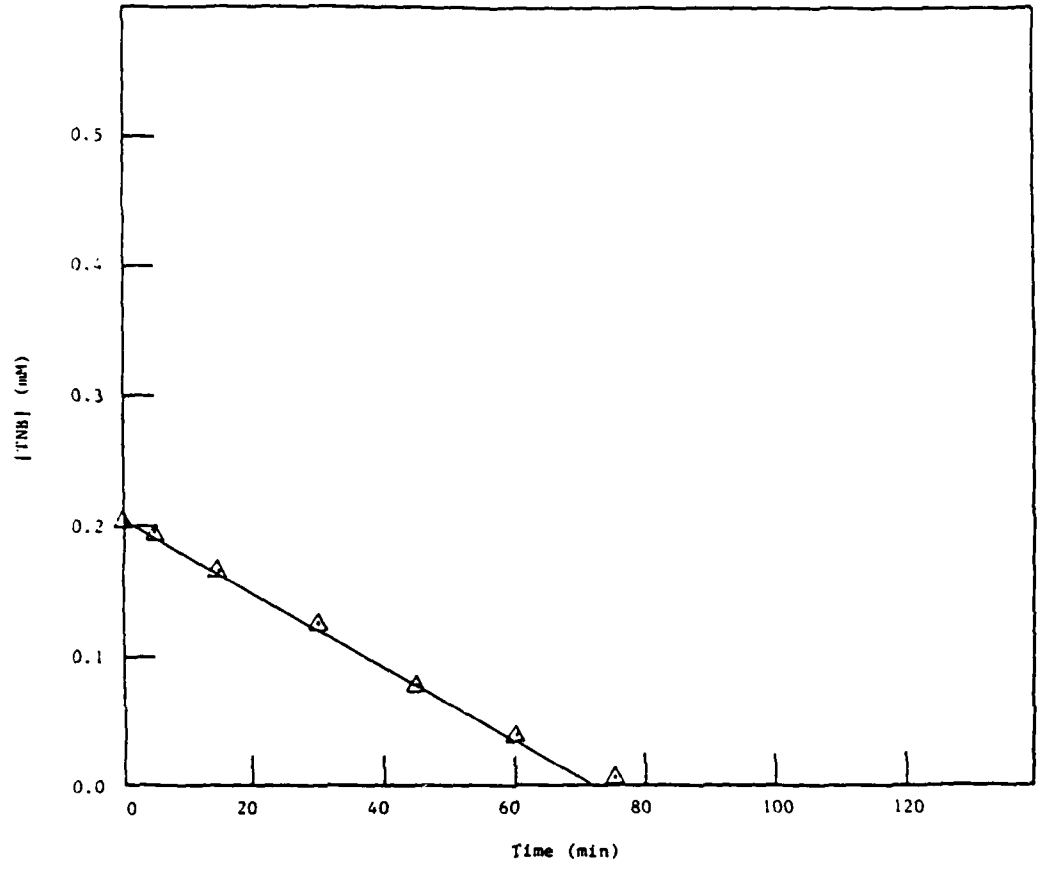

Figure B-7. Concentration of TNB versus time with ozone and photolysis at high temperature (67°C).

$[TNB]_0$ = 0.2 mM

Ozone dose rate = 6.6×10^{-6} $M \cdot s^{-1}$

I = 1.31 W/02.L

Temp. = 67°C

pH_0 = 1.79

pH_f = 1.74

APPENDIX C

List of Symbols

A	=	absorbance
Ac^-	=	acetate ion
$(Ac^-)_{ox}$	=	acetate oxidation products
BKI/M	=	boric acid buffered KI/ammonium molybdate method
C	=	concentration
HBI	=	Hoigne-Bader indigo method
I	=	light intensity
k	=	reaction rate constant
$[O_3]_{dose}$	=	O_3 dose rate in solution
pH_f	=	final pH
pH_o	=	initial pH
R	=	reaction rate
S	=	substrate
SMG	=	sulfite-Meissenheimer colorimetric method for TNT and TNB
TOC	=	total organic carbon
T_f	=	final solution temperature
T_o	=	initial solution temperature
α	=	yield of TNB removal per O_3 molecule
E	=	molar extinction coefficient
η	=	reaction quantum yield
λ	=	wavelength of light
Φ_o	=	quantum yield for decomposition of O_3 by UV light
$\Phi_{\cdot OH}$	=	hydroxyl radical yield